

RESEARCH

Open Access



Fabrication and evaluation of smart pH/thermo dual-responsive injectable intratumoral in situ depot hydrogels for controlled 5-FU delivery

Samiullah Khan^{1*}, Bangul Khan^{2,4} and Huan Li^{1,3}

Abstract

Background 5-FU has multiple applications in various cancers but has limitations owing to its shorter half-life and rapid metabolism. In this study, injectable intratumoral gels were developed to enhance 5-FU concentrations in tumor vicinity. Sterile tunable poly (N-isopropylacrylamide)-based pH/thermo dual-sensitive self-assembled and in situ crosslinkable injectable depot gels with low viscous grade of chitosan (LVCS) were developed via cold and free radical polymerization method for localized and sustained delivery.

Results Rheological analysis confirmed the gelation temperature, sol–gel transitions and viscoelastic behavior of in situ gels. Swelling–deswelling–reswelling cycles established the effect of temperature on structural changes. Swelling tests and in vitro drug release conducted in various dissolution media at variable temperatures confirmed pH/thermal dual response of formulations. Methyl thiazolyl tetrazolium assay confirmed that the hydrogels have good cytocompatibility with above 85% cells viability in Vero cells. In vitro cytotoxicity assay against MCF-7 cells displayed that 5-fluorouracil has good anticancer activity in loaded gel form as compared to free 5-FU. The cytotoxic studies showed that IPLVCS-2 and IPLVCS-6 have the highest inhibition ($IC_{50} = 47 \pm 1 \mu\text{g/ml}$, $34 \pm 17 \mu\text{g/ml}$) as compared to free 5-FU ($IC_{50} = 52 \pm 3 \mu\text{g/ml}$).

Conclusion Current findings conclude that taking the advantage of physiologic environment acidic pH and high temperature of cancer cells, poly(NIPAAm)-g-LVCS formulations can effectively be used as intratumoral controlled depot of 5-FU.

Keywords Dual-responsive gels, Intratumor depot, 5-Fluorouracil, MCF-7 cancer cells, Low viscous chitosan, Vero cell lines, N-Isopropylacrylamide

*Correspondence:

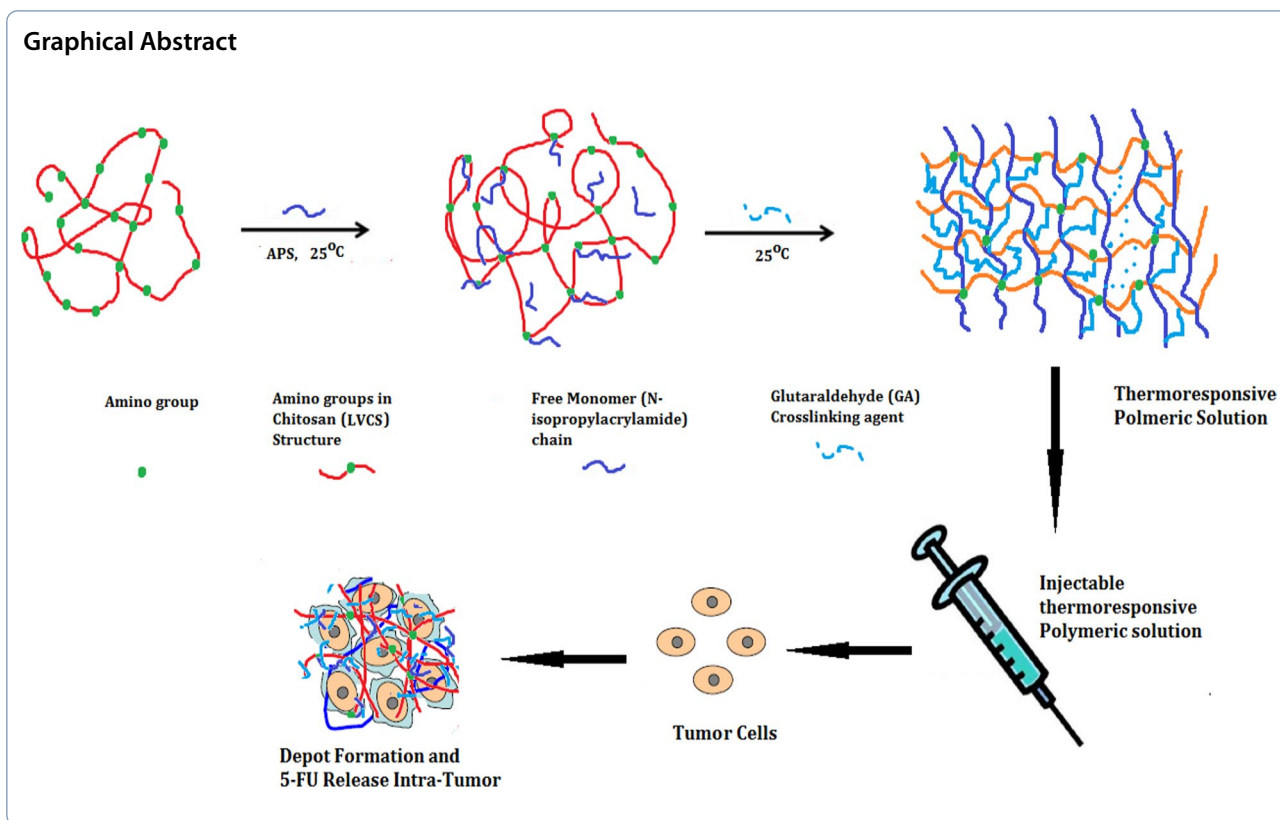
Samiullah Khan

Sami_pharmacist99@hotmail.com

Full list of author information is available at the end of the article



© The Author(s) 2023. **Open Access** This article is licensed under a Creative Commons Attribution 4.0 International License, which permits use, sharing, adaptation, distribution and reproduction in any medium or format, as long as you give appropriate credit to the original author(s) and the source, provide a link to the Creative Commons licence, and indicate if changes were made. The images or other third party material in this article are included in the article's Creative Commons licence, unless indicated otherwise in a credit line to the material. If material is not included in the article's Creative Commons licence and your intended use is not permitted by statutory regulation or exceeds the permitted use, you will need to obtain permission directly from the copyright holder. To view a copy of this licence, visit <http://creativecommons.org/licenses/by/4.0/>.



1 Background

Cancer is nowadays the leading public health problem all around the globe. In the USA, one in every four deaths occur due to cancer. Chemotherapy for cancer has always been remained a challenging job [14]. Various treatment strategies have been introduced for cancer chemotherapy. The efficiency of chemotherapeutic agents has often been inadequate by the exposure of healthy cells to the serious side effects of these anticancer agents [26, 40]. Surgical removal of tumor is the primary clinical treatment, but complete removal was not achieved successfully. Therefore, in most cases, to kill the malignant cells and to prevent tumor reoccurrence, surgery is followed by systemic chemotherapy or irradiation to remove the remaining tumor cells. However, owing to concurrent excretion, systemic chemotherapy leads to lesser distribution to target tissue [9, 24], because the non-specific distribution of cancer drugs to healthy tissues caused severe toxic effects [12].

5-Fluorouracil (5-FU), a pyrimidine analogue, which interferes with thymidylate synthesis is one of chemotherapeutic compounds that has application in many solid tumors such as breast cancer [40], gastric cancer [26], pancreatic cancer [9] and colorectal cancer [24]. Limitations to 5-FU include rapid metabolism by dihydropyrimidine dehydrogenase owing to short plasma

half-life, ununiform and poor oral absorption and damage of the healthy cells due to its non-selectivity. To increase the efficacy of the 5-FU and to retain the drug in the general circulation for longer time during the entire treatment period remained the desirable goal for many years. So, to achieve this objective, the carrier system needs to be modified [4].

Intelligent biopolymer systems which are also known as “materials with brain” with capability of in situ gel forming have recently gained an increasing importance and interest of researchers in developing biosensors and drug delivery carriers. These systems have the potential to detect a minute change and show response to the external or internal factors such as pH [29], temperature [3], light [22], ionic strength and magnetic field [28]. Due to identical human body environment with some of these factors, pH/temperature-responsive hydrogels have been widely studied which can be simply and easily controlled both in vitro and in vivo [19].

Hydrogels with 3D network are the superabsorbent which have the ability to absorb high amount of water and biological fluids. Injectable hydrogels with biodegradable and biocompatible nature undergo a temperature-induced phase transition and form a depot system in situ. These injectable in situ hydrogels are formed after injection via sol–gel phase transition or via in situ

chemical polymerization which have gained extensive interest as an emerging platform and have been widely investigated. Such thermoresponsive depot systems which do not need the use of any type of polymerization agents, externally applied triggering agents, or organic solvents have discovered huge biomedical applications as matrices in tissue engineering, drug delivery and cell carriers [5, 20, 21]. These polymeric matrices following gelation act as site-specific depots for the delivery of pharmaceuticals [27]. To overcome the problem associated with cancer treatment, an alternative approach is to encapsulate the chemotherapeutic agent in biodegradable and biocompatible thermosensitive polymeric solution that can be injected either locally to deliver the drug at tumor site or injected through subcutaneous route. After injection the thermoresponsive solution will undergo *in situ* polymerization and will convert into a depot form in response to normal physiological body temperature. In the past (for last 5 years), a very few articles have been reported for the delivery of 5-FU via injectable hydrogels. Lin et al. [41, 42] prepared *N*-isopropylacrylamide-based hydrogels with carboxymethyl chitosan for the delivery of 5-FU. Moreover, no work has been reported with low viscous chitosan in the literature with *N*-isopropylacrylamide for 5-FU delivery. Additional file 1: Fig. S1 indicates the general illustrations of pH, temperature and pH/Thermo dual responsive hydrogels.

During last few decades, biopolymers from natural and synthetic sources have been widely utilized to prepare injectable scaffolds as drug and gene delivery carrier owing to excellent biodegradable and biocompatible nature [20, 21].

Low viscous chitosan (LVCS) is a cationic synthetic derivative of natural chitosan, which is formed from *N*-deacetylation of chitin. It is a linear polysaccharide of β -(1–4)-linked 2-acetamido-2-deoxy-D-glucopyranose and 2-amino-2-deoxy-D-glucopyranose units. It has found successful applications in tissue engineering and drug delivery owing to nontoxic, biodegradable, biocompatible, excellent swelling and pH-sensitive properties [18]. However, LVCS has only solubility in acidic solution and has greatly limited its applications [8, 24].

Poly (*N*-isopropylacrylamide) (PNIPAAm), temperature-responsive polymer, acts as a best suitable candidate for the development of injectable hydrogels. This polymer has reversible volume phase transition at its lower critical solution temperature (LCST) between 30 and 32 °C close to body temperature [7]. Below LCST, PNIPAAm chains become hydrated in water, which leads to the formation of expanded structure, while above LCST, a compact structure is formed due to water loss [6]. The phenomenon of this structural transition changes the permeability of the gel network, which can be utilized to

switch the release of the pharmaceuticals “on and off” in the delivery devices [36].

Tumor has a slightly acidic atmosphere with high temperature as compared to normal body cells and tissues [37–39]. The lower pH of tumor tissues is because of the high glycolytic activity that produces acids equivalents in cells, while tumor tissues have slightly higher temperature because of continuous replication, which needs and releases energy. The increased temperature of tumor cells is also suggested to be due to the increased glycolytic flux [2].

Keeping in mind these environmental conditions, our group has reported intratumor dual-responsive pH/thermo injectable depot gels of PNIPAAm with low viscous chitosan through self-assembling and *in situ* chemical polymerization techniques in this study. The study aimed that pH/thermo dual-responsive formulations will respond to acidic pH and high temperature locally in the tumor vicinity. The formulations will undergo sol–gel transition, form a local drug depot and will release the drug in controlled manner. As per literature review, no work with LVCS has been reported targeting the intratumor environment. Herein in this study we reported a detailed study representing pH/thermo dual nature based on LVCS and NIPAAm for intratumoral applications. The developed gels were screened for sol–gel phase change, gelation time, optical transmittance and temperature-induced changes, viscosity determination, rheological properties and swelling characterization at various pH and temperatures. For developed depot gels, networking parameters were calculated using Flory Huggins theory. *In vitro* drug release and anticancer activity of these injectable depot formulation were further investigated using MTT (Methyl thiazolyl tetrazolium) assay. Structural and thermal analysis of the selected samples was conducted via nuclear magnetic resonance (NMR), Fourier transform infrared spectroscopy (FTIR), thermogravimetric analysis (TGA), differential scanning calorimetry (DSC) and scanning electron microscopy (SEM). Current findings indicate that shortcomings associated with 5-FU can effectively be overcome by encapsulating in pH/thermo dual-responsive gels. Moreover, the development of these dual-nature formulations can be applied locally for effective treatment in various cancer types taking the advantage of tumor local conditions. Additionally, we are confident that the development of these dual-nature formulations will provide an alternative hallmark in the biomedical field.

2 Methods

2.1 Materials

Low viscous chitosan (Average M_w = 45,000–60,000) (Sigma-Aldrich), *N*-isopropylacrylamide (NIPAAm, 99%

purity) (Sigma-Aldrich), 5-fluorouracil (99%) (Sigma-Aldrich), ammonium persulfate, glutaraldehyde (GA), acetic acid, sodium dihydrogen phosphate, sodium hydroxide, sodium chloride (ABCAM), and deionized water were used for conducting experiments.

2.2 Preparation of self-assembled and chemically crosslinked in situ gel formulations

The injectable thermosensitive self-assembled and chemically crosslinked *in situ* depot gels were synthesized by cold and free radical polymerization method. The polymers and other reaction parameters used in various feed composition ratio are given in Table 1.

2.2.1 Self-assembled in situ gel formulations

Briefly, weighed quantity of NIPAAm was stirred at 300 RPM in cold distilled water alone as per composition shown in Table 1. NIPAAm dispersion was kept at 4 °C for 24 h till clear NIPAAm solution obtained. The final sample was stored in sterilized glass vials for further studies [25].

2.2.2 Chemically crosslinked in situ gel formulations

2.2.2.1 Preparation of poly (LVCS-grafted-NIPAAm) in situ gel formulations A similar procedure as described above was adopted for the preparation of poly (LVCS-grafted-PNIPAAm) injectable hydrogels via free radical polymerization technique with minor modifications [15]. LVCS was dispersed in 1% acetic acid under at 300 RPM for 30 min as per feed ratios given in Table 1. NIPAAm was dissolved in cold distilled water and then stored at 4 °C for 24 h to obtain clear solution after filtration (0.45 micron). Ammonium persulfate previously sterilized by autoclaving in an appropriate quantity was added to NIPAAm solution. The grafting reaction was conducted by the dropwise addition of NIPAAm solution into LVCS solution under nitrogen atmosphere at room temperature. Glutaraldehyde in various concentrations was finally added to mixture and the final solution was

stirred for 30 min. The final co-solution was placed at 4 °C in sterilized glass vials for further studies. Figure 1 shows the proposed poly (LVCS-g-NIPAAm) injectable depot hydrogels structure.

2.2.3 Characterization of in situ gels

2.2.3.1 ¹H and ¹³C nuclear magnetic resonance (NMR) analysis To confirm the copolymer structure, ¹H and ¹³C NMR spectra of NIPAAm, LVCS, and poly (LVCS-g-PNIPAAm) samples were noted in DMSO as solvent on 400/Varian VXR 200 spectrometer. The chemical shifts were characterized in parts per million (ppm), and tetramethylsilane (δ=0 ppm) was used as internal standard [44].

2.2.3.2 FTIR analysis FTIR of pure NIPAAm, pure LVCS, 5-FU, IPLVCS copolymer (IPLVCS-2) and samples were recorded under 4000–400 cm⁻¹ using KBr pellets in 1:100 proportions on FTIR spectrophotometer (Tensor-II BRUKER USA) [41, 42].

2.2.3.3 TG analysis Thermogravimetric analyzer (DTG 60, Shimadzu, Japan) was used to analyze thermal stability of samples. Decomposition peaks were recorded between 25 and 1000 °C at 20 °C/min under nitrogen gas flow of 30 ml min⁻¹ [33].

2.2.3.4 DSC analysis Netzsch DSC 204 F1 Phoenix thermal apparatus was used to carry out the thermal analysis of the gels. Samples (5 mg) were placed in an aluminum holder and heated under 25–1000 °C at 20 °C/min [33].

2.2.3.5 SEM analysis The porosity of poly (LVCS-g-NIPAAm) hydrogels was monitored using SEM (JSM-6490A, Japan). Dried hydrogel disks were powdered, mounted on an aluminum stub and scanned at 20 kV with 0.6 mm Hg chamber pressure and variable magnification [32].

Table 1 Feed ratios of synthesized poly (LVCS-g-PNIPAAm) gels (n=3)

Codes	PNIPAAm (g)	LVCS (g)	APS (g)	GA (g)	T _{sol-gel} (°C)	Gelation time (G _T)	H ₂ O (g)
IP-1	0.500	–	–	–	37	No gelation	10 g
IP-2	1	–	0.020	–	34±0.21	~ 17 min	10 g
IP-3	1.5	–	0.020	–	34±0.20	~ 10 min	10 g
IPLVCS-1	1	0.150	0.015	0.015	35±0.23	~ 8 min	10 g
IPLVCS-2	1	0.200	0.015	0.015	35±0.27	~ 10 min	10 g
IPLVCS-3	1.5	0.200	0.015	0.015	34±0.90	~ 07 min	10 g
IPLVCS-4	2.0	0.200	0.015	0.015	33±0.20	~ 06 min	10 g
IPLVCS-5	2.5	0.200	0.015	0.020	34±0.05	~ 04 min	10 g
IPLVCS-6	2.5	0.200	0.015	0.025	33±0.60	~ 02 min	10 g

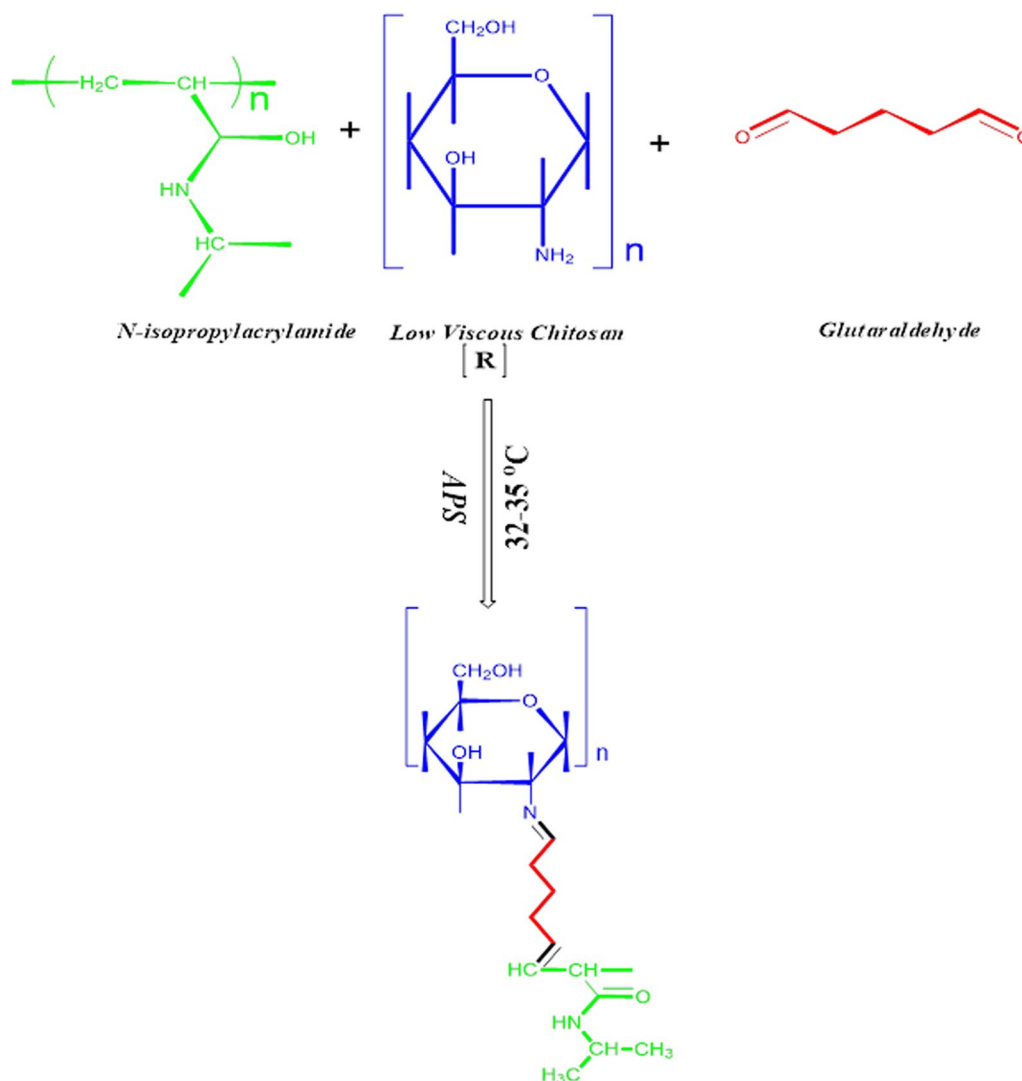


Fig. 1 Proposed structure of poly (LVCS-g-PNIPAAm) pH/thermo dual-responsive in situ injectable depot hydrogel. APS was used as initiator, while glutaraldehyde (GA) was used as crosslinking agent

2.2.4 Clarity of formulations

The clarity of polymeric solutions and *in situ* formed gels was visually monitored at 4 °C, 25 °C and 37 °C.

2.2.5 Phase diagram measurement of formulations (Tsol-gel)

The phase transition temperature of all samples was monitored by tube inverting method [25]. Each time stated in Table 1, 3 ml sample was taken in test tube, sealed with parafilm and retained in digital water bath maintained at gelation temperature. Each minute, per °C temperature was increased after solutions equilibration to confirm the gelation temperature. The gelation of solution was confirmed by titling test tube at 90°.

2.2.6 Determination of viscosity of formulations

The steady shear viscosity of all samples was determined by Digital Brookfield Viscometer. A 25 ml sample was taken in a beaker using spindle 52 at room temperature. A shear rate (spindle speed) in the range of 0.3–60 rpm was applied. All the samples were analyzed in triplicates for accuracy of results [41, 42].

2.2.7 Rheological analysis

For the analysis of rheological properties, the poly (LVCS-g-NIPAAm) copolymer solutions were prepared in their respective solvents at different polymeric and crosslinker concentrations. The rheological behavior of the in situ injectable gel samples was monitored via time sweep experiments over 20–37 °C using AR-2000

rheometer at 1 rad/s oscillatory frequency fixed with 40 mm plate. The gelation mechanism was noted by calculating storage (G') and loss (G'') moduli over 300 s [16].

2.2.8 Measurement of optical transmittance

Optical transmittance of poly (LVCS-g-NIPAAm) gels was monitored at diverse temperatures at 450 nm. The transparencies of samples were observed using disposable curettes in digital water bath. Temperature was changed from 25 to 45 °C and retained at specified temperature for 5 min prior to analysis [23, 35].

2.2.9 Swelling test

The swellability of poly (LVCS-g-NIPAAm) hydrogels was analyzed with respect to phosphate buffer solution (PBS, 5 mM, pH=7.4), distilled water and (pH=2.1) at 25 °C, 37 °C and 45 °C in closed containers. For swelling tests, the hydrogel samples were cut into 8×8 mm disks. At specific time intervals, samples were withdrawn from respective solution, blotted with paper prior to weigh and reverted back to solution till equilibrium value obtained. The following formula was used for swelling ratio calculation [34],

$$\text{Swelling Ratio(SR)} = \frac{W_s - W_d}{W_d} \tag{1}$$

where W_s is swollen gels weight and W_d specifies dry weight.

2.2.9.1 Oscillatory swelling tests Poly (LVCS-g-PNIPAAm) hydrogels were tested for oscillatory swelling–deswelling–reswelling cycles in buffer solutions of pH=2.1 at various temperatures. Briefly, hydrogel disks were dipped in buffer for 2 h at 25 °C and then kept in solution at 37 °C for 2 h and repeat again. Each time, swollen sample weight was observed before each immersion. Oscillatory cycles were determined at different pH values by same method reported earlier [34].

The swelling ratio (SR) was calculated by using Eq. 1.

2.2.9.2 Diffusion coefficient (D) Drug release from poly (LVCS-g-PNIPAAm) hydrogels generally occurs via diffusion. Diffusion coefficient (D) denotes substance passes in unit time across concentration gradient through unit area. For “ D ” measurement, dried disks were saturated at pH=2.1. “ D ” values were measured by the following formula [17]:

$$D = \pi \left(\frac{h \cdot \theta}{4 \cdot Q_{eq}} \right) \tag{2}$$

where D denotes diffusion coefficient, Q_{eq} is equilibrium swelling degree, θ is slope of the linear part of the swelling curves, and h is initial dry gels thickness.

2.2.10 Network parameters of pH/thermo dual-responsive injectable depot hydrogels

2.2.10.1 Molecular weight between crosslinks (Mc) Rehner theory was used for determining Mc values of hydrogels. Mc values were determined by the following formula [17]:

$$Mc = - \frac{d_p v_s \left(v_{2,s}^{1/3} - v_{2,s}/2 \right)}{\ln \left(1 - v_{2,s} \right) + v_{2,s} + \chi v_{2,s}^2} \tag{3}$$

2.2.10.2 Polymers volume fraction ($v_{2,s}$) Polymers volume fraction ($v_{2,s}$) refers to absorbing ability of hydrogel sample. The following formula was used for the calculation of ($v_{2,s}$) of samples:

$$v_{2,s} = \left[1 + \frac{d_h}{d_s} \left(\frac{M_a}{M_b} - 1 \right) \right]^{-1} \tag{4}$$

where d_h and d_s are densities (g/ml) of the gel and solvent. M_a and M_b are masses (gm) of sample in swollen and dry state [1].

2.2.10.3 Solvent interaction parameters (χ) The gels components compatibility with the surrounding liquids was measured via solvent interaction parameters. χ values were calculated by the following equation:

$$\chi = \frac{\ln \left(1 - v_{2,s} \right) + v_{2,s}}{v_{2,s}^2} \tag{5}$$

where $v_{2,s}$ (ml/mol) denotes swollen gels volume fraction [1].

2.2.11 Grafting efficiency

The amount of grafted NIPAAm to LVCS was calculated by method reported by Zhang et al. [41, 42]. The percentage grafting efficiency was calculated using the following formula:

$$\text{Grafting efficiency \% (GE)} = \frac{W_g - W_{cs}}{W_m} \times 100 \tag{6}$$

where W_g , W_{cs} and W_m represent weights of grafted copolymer, LVC and NIPAAm.

2.2.12 Determination of percent crosslinking

Percent crosslinking of dried xerogel disks was determined by placing distilled water (50 ml) at 25 °C. The gels were stirred for 24 h to remove the unbind form. Disks were kept on drying at 37 °C till regular weight. Percent crosslinking was determined using the following formula [13]:

$$\% \text{ Crosslinking} = \frac{W_2}{W_1} \times 100 \tag{7}$$

W_1 and W_2 specify the weights of dried disks prior and post procedure.

2.2.13 Drug loading by soaking method

5-Flourouracil (5-FU) was selected as model drug for loading in poly (LVCS-g-PNIPAAm) hydrogels. Swelling diffusion/soaking method was adopted for loading of the model drug. Loading of model drug in chemically crosslinked in situ hydrogels was carried out in samples with highest swelling. A 1% 5-FU solution was prepared in distilled water. Dried hydrogel disks of selected samples were soaked in 5-FU (100 ml) of solution at 25 °C. The weight of the disks was checked regularly until equilibrium swelled weight was obtained that allow maximum drug uptake. After equilibrium value, the samples were dried at 40 °C [18].

2.2.14 Measurement of 5-FU loading

For drug loading efficiency measurement of poly (LVCS-g-PNIPAAm) in situ gels, extraction method was used. Each time 25 ml of fresh DW was used for extracting entrapped drug. This process was continued till no drug contents were left in the solution. Drug contents in pooled extract were determined using UV–Visible spectrophotometer at 265 nm [18].

2.2.15 In vitro drug release experiments from poly (LVCS-g-PNIPAAm) gel formulations

The *in vitro* drug release was monitored using USP apparatus-II in DW, PBS (pH=7.4) and pH=2.1 respectively at different temperatures. The drug-loaded samples were soaked in containers at designated pH and labeled temperature. At fixed interval, 2 ml sample was taken out and analyzed for drug contents at 265 nm. The bath conditions were kept constant by replacing with fresh media. Results were expressed as cumulative percentage release using a standard calibration curve constructed in appropriate ranges [10].

2.2.16 Drug release kinetics

The kinetics of release was assessed by applying different models [18].

Zero model

$$Q_t = Q_0 + K_0t \tag{8}$$

Q_t indicates dissolved drug in time t , and Q_0 is the initial drug. K_0 is constant.

First model

$$\ln M_t = -k_1t + \ln M_0 \tag{9}$$

M_0 is original drug, and M_t is the leftover drug. K_1 is constant.

Higuchi model

$$M = k_Ht^{1/2} \tag{10}$$

where M is drug released at t and kH is constant.

Korsmeyer–Peppas model

$$\ln (M_t/M_\infty) = \ln k_p + n \ln t \tag{11}$$

(M_t/M_∞) is drug fraction released t , and n refers to slope showing release mechanism from the gels structure.

2.2.17 Cell lines and cell culture

For the *in vitro* cell cytotoxicity/compatibility studies, breast (MCF-7) cancer and Vero cells were cultured in growth medium containing RPMI-1640 supplemented penicillin (100 U mL⁻¹), streptomycin (100 µg mL⁻¹), l-glutamine (2 mM) and 10% FBS and stored at 37 °C in an incubator supplied with 5% CO₂.

After 90% confluency obtained, the cells were separated and then resuspended in growth medium for further use [30].

2.2.17.1 Methyl thiazolyl tetrazolium (MTT) assay The relative cytotoxicity and cytocompatibility were assessed by MTT viability assay against MCF-7 and Vero cells previously seeded in 96-well plate at 10,000 cells/well. The cells were applied 100 µl of pure 5-FU solution, copolymer solutions containing encapsulated 5-FU and blank copolymer solutions and incubated at 37 °C for 24 h. During incubation, samples solution changed from sol to gel state forming drug-loaded depot. The untreated cells alone served as negative control, and Triton X100 was used as positive control. The absorbance was calculated on Bio-Rad 680 microplate reader at 570 nm. Cells (%) viability was measured by the following equation [30]:

$$\text{Cells Viability \%} = \frac{A_{\text{sample}}}{A_{\text{control}}} \times 100 \tag{13}$$

A_{sample} and A_{control} show absorbance of sample and control wells.

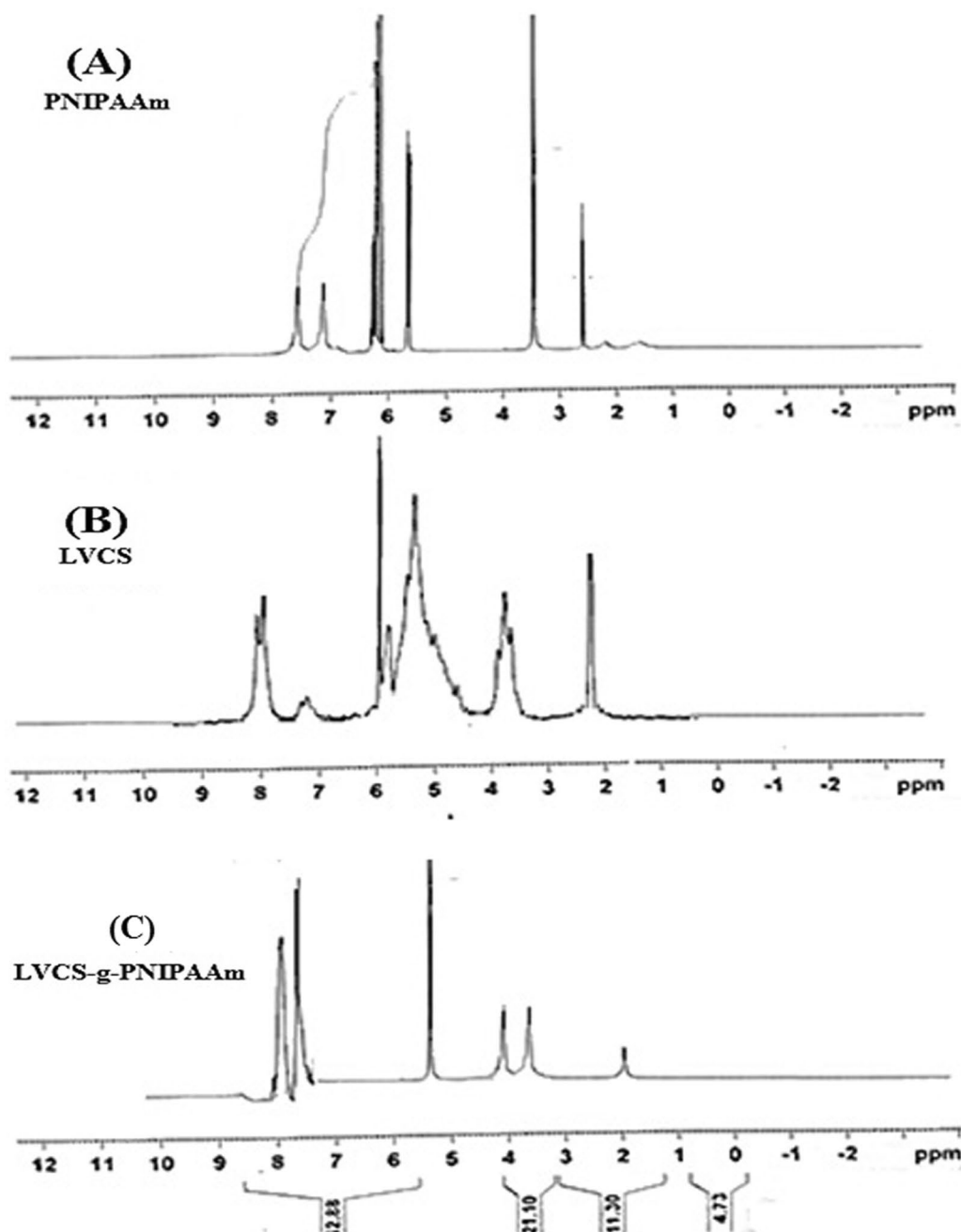


Fig. 2 ¹H NMR of **A** PNIPAAm, **B** LVCS and **C** poly (LVCS-g-PNIPAAm) gel

2.3 Statistical analysis

Results are presented as percentage or mean ± SD. Results were statistically tested for significance by ANOVA using GraphPad InStat. Statistically significant values were defined as $P < 0.05$.

3 Results

3.1 Instrumental analysis

3.1.1 NMR analysis

¹H and ¹³C NMR spectrums of PNIPAAm, LVCS and poly (LVCS-g-PNIPAAm) are shown in Figs. 7 and 8, respectively.

In ¹H NMR of PNIPAAm shown in Fig. 2A, peak at 2.59 ppm was assigned to CH₃ group, while peak at 3.61 ppm indicates the N-CH-. Peak at 5.68 ppm and group of peaks at 6.11 ppm were assigned to

CH₂=CH- groups demonstrating various protons atoms. Additionally, peaks at 7.22–8.0 ppm were assigned to NH- groups. In ¹³C NMR spectrum of PNIPAAm shown in Fig. 3A, the clustered peaks in the range of

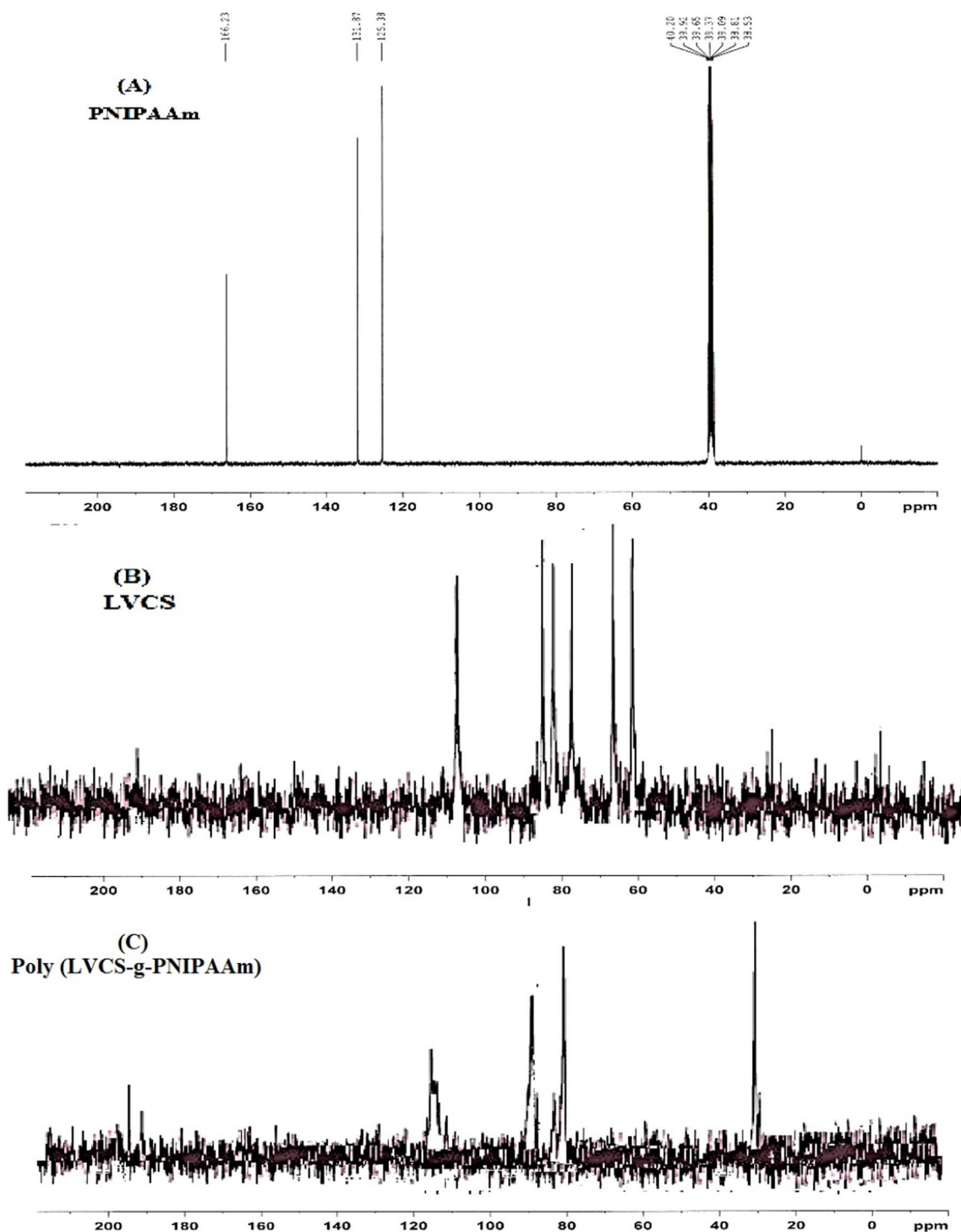


Fig. 3 ¹³C NMR of A PNIPAAm, B LVCS and C poly (LVCS-g-PNIPAAm) sample

38.63–40.30 ppm refer to CH– (in side chain). The peaks appeared at 125.45 ppm and 131.96 ppm were assigned to C in NC– group (main chain). Peak at 166.31 appeared was assigned to carbon atom in (C=O).

In ^1H NMR of LVCS shown in Fig. 2B, the signal at 1.99 ppm was attributed to proton position of $-\text{CH}_3$ from acetamido group. The peaks appeared between 2.85 and 3.13 ppm were assigned to hydrogen atoms bonded to the carbon C2 of the glucosamine ring. The signals between 3.58 and 3.92 ppm correspond to the hydrogens attached to carbon atoms (C3, C4, C5 and C6) of the glucopyranose. The signal appeared in the range of 4.75 and 5.07 ppm was allocated to the hydrogen bonded to C1. The ^{13}C NMR of the LVCS shown in Fig. 3B indicates the signals at 26 ppm and 178 ppm which corresponds to the C of methyl group ($-\text{CH}_3$) and carbonyl carbon of ($-\text{COCH}_3$). The signals appeared at 60.11 ppm, 72.13 ppm, 82 ppm, 78.4 ppm and 65 ppm correspond to the C2, C3, C4, C5 and C6 of glucopyranose respectively. The signal at 112.10 ppm is attributed to the C1 of the chitosan.

The ^1H NMR spectrum of poly (LVCS-g-PNIPAAm) in Fig. 2C also indicates the introduction of some new signals appeared at 2.56 ppm and 3.22 ppm which are assigned to CH_3 group and N-CH– group from PNIPAAm, respectively. This indicates that PNIPAAm was successfully grafted on the LVCS backbone.

The ^{13}C NMR of poly (LVCS-g-PNIPAAm) gel sample presented in Fig. 3C shows the appearance of shifted signal at 31.90 ppm which corresponds to the CH– group from NIPAAm. Moreover, the absence of signals in the region of 80–100 ppm corresponds to the grafting reactions.

3.1.2 FTIR analysis

The FTIR spectra of PNIPAAm, LVCS and IPLVCS-2 copolymer hydrogel samples are shown in Fig. 4. Peak at 1617 cm^{-1} was attributed to the carbonyl amide and N–H stretching of NIPAAm. Peaks appear at $\sim 1423\text{ cm}^{-1}$ and $\sim 1456\text{ cm}^{-1}$ attributed to the absorbance of isopropyl in NIPAAm as shown in Fig. 4A. In FTIR of LVCS shown in Fig. 4B, absorption peak appears between ~ 3000 and 3300 cm^{-1} mainly allocated to the O–H stretching. The peak at $\sim 2900\text{ cm}^{-1}$ was attributed to the C–H stretching in $-\text{CH}_2$. Peaks at $\sim 1575\text{ cm}^{-1}$ and $\sim 1624\text{ cm}^{-1}$ are mainly allocated to C–O stretching in secondary amide, amide I and amide II. The peak appears at $\sim 1322\text{ cm}^{-1}$ is mainly attributed to $-\text{C}-\text{N}$ stretching in secondary amide and amide III. The peak at $\sim 1250\text{ cm}^{-1}$ is attributed to C–O stretching of ring ether. Peak in the range of ~ 3400 – 3500 cm^{-1} was assigned to characteristics amino group ($-\text{NH}_2$ group) often marked by the broad OH absorption. Figure 4C shows the FTIR of 5-FU. In spectrum of

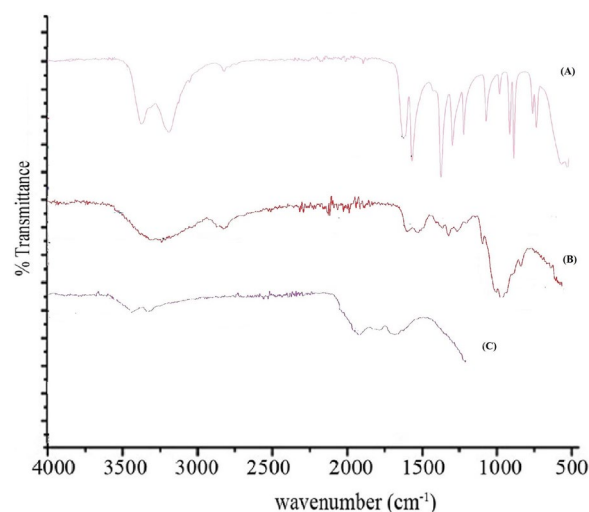


Fig. 4 FTIR spectra of **a** Pure PNIPAAm, **b** Pure LVCS and **c** IPLVCS-2 copolymer hydrogel

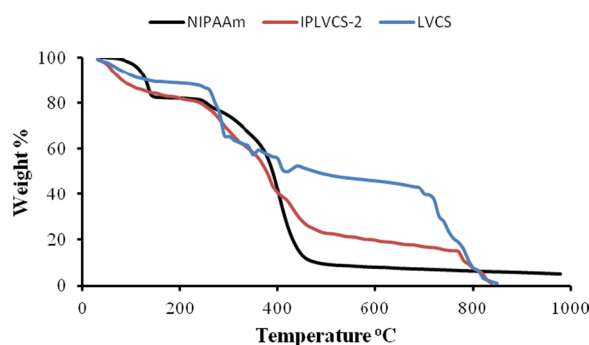


Fig. 5 Thermogravimetric analysis of PNIPAAm, pure LVCS and IPLVCS-2 copolymer hydrogel

poly (LVCS-grafted-NIPAAm) (IPLVCS-2) shown in Fig. 9D, peak at $\sim 1617\text{ cm}^{-1}$ attributed to amide group in NIPAAm and peak at $\sim 2903\text{ cm}^{-1}$ assigned to $-\text{CH}(\text{CH}_3)_2$ groups show that NIPAAm was grafted onto LVCS chain. Moreover, from the FTIR spectra of copolymer hydrogels, crosslinking with glutaraldehyde has been confirmed. In the crosslinking reaction with glutaraldehyde there is a simultaneous drop in various bands compared with spectra of pure LVCS, which indicates the evidence of interaction between functional groups.

3.1.3 TG analysis

The thermal stabilities of NIPAAm, LVCS and IPLVCS-2 are presented in Fig. 5 using TG analysis under N_2 atmosphere. The sample IPLVCS-2 was selected for studying the thermal stabilities based on their high molecular weight and feed ratio composition (10: 2).

For pure PNIPAAm, the decomposition peak was noted at $185\text{ }^\circ\text{C}$ which is increased to $230\text{ }^\circ\text{C}$ and ends at

410 °C. In TG analysis of LVCS, the maximum degradation temperature (first derivative peak of temperature) was observed at 250 °C, and after increasing to 270 °C, it ends at 310 °C. The TG spectra of copolymer sample (IPLVCS-2) exhibit two-stage thermal decomposition behavior. For copolymer sample, the first degradation peak was seen in range of 240 °C and the second was noted at 480 °C. The first stage decomposition was supposed to be due to chitosan chains decomposition, and the second stage was supposed to be NIPAAm chain decomposition. The observation of the two-stage degradation confirms the grafting reaction between the copolymer hydrogel. Moreover, this behavior also specifies the thermal stability of the graft copolymer hydrogel in comparison to pure NIPAAm and polymer (LVCS).

3.1.4 DSC analysis

DSC thermograms of pure PNIPAAm, LVCS and IPLVCS-2 copolymer gels are displayed in Fig. 6.

DSC of pure PNIPAAm shows that the initial endothermic peak starts from 30 °C and goes to a peak point at 90 °C. This endothermic transition of pure PNIPAAm is near to the phase transition temperature (LCST) of PNIPAAm (32 °C), which is attributed to hydrophobic hydration of the isopropyl groups of PNIPAAm. The DSC of NIPAAm shows various exothermic peaks that starts from 170 °C and ends at 700 °C suggesting degradation of monomer at elevated temperature.

DSC of pure LVCS shows an endothermic peak starts from 42 °C and ends at 80 °C. Moreover, it also shows exothermic peaks. One peak starts from 80 °C and reach to peak position of 290 °C, while it shows an exothermic maxima at 500 °C. This may be related to decomposition of glucose amine units with correspondence to exothermic peaks.

In case of IPLVCS-2, a slight variation in the transition temperature for formulations with respect to pure NIPAAm has been observed. For IPLVCS-2, the

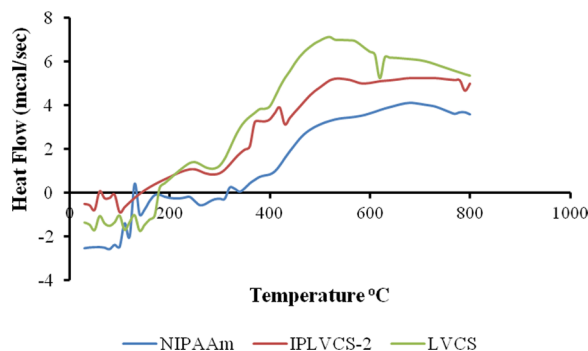


Fig. 6 DSC thermograms of pure PNIPAAm, pure LVCS and IPLVCS-2 copolymer hydrogel

endothermic peak starts at 35 °C and reaches peak position of 80 °C. The exothermic maxima for IPLVCS-2 hydrogel was noted at 570 °C. This change in transition temperature might be due to the hindrance created by polysaccharide chains on the mobility. This is also attributed to be due to grafting and molecular entanglements of NIPAAm chains. However, the initial transition temperature for copolymer smart hydrogel lies within the range of human body temperature. This also shows that no critical significant change was observed for smart hydrogel samples in the phase transition temperature.

3.1.5 SEM analysis

Figure 7 shows the surface and internal morphologies of hydrogel samples. SEM micrograph at different resolutions clearly indicates the highly porous nature of copolymer hydrogel. It is hypothesized that these pores highly facilitate water penetration and release of 5-FU in and outside of gel structure. The size of these micropores ranged between 20 and 50 μm in diameter.

3.2 Clarity of the in situ gels

The polymeric solutions and gels reported in Table 1 were monitored visually for clarity. The developed gels were also found to be transparent at diverse temperatures representing the solubility of all components.

3.3 Phase diagram measurement of formulations (Tsol-gel)

Table 1 indicates the phase transition temperatures and gelation time of in situ gel formulations. The developed formulations include PNIPAAm-based formulations alone and in combination with low viscous chitosan (LVCS). The sample IP-1 has shown no conversion from sol-gel at the PNIPAAm concentration of 0.500 g. However, with increase in concentration, phase change from solution to gel state was observed in the physiologic temperature range. All the rest of the formulations show a transition temperature at physiological temperature in the range of 32–37 °C. Table 1 also indicates the gelation time of the gels. Figure 8 indicates the phase change of in situ gels from sol-gel state.

3.4 Viscosity determination

For the determination of viscosity of the copolymer solutions, DV1-Prime Digital Brookfield viscometer was used.

3.4.1 Effect of spindle speed

To evaluate the effect of spindle speed on viscosity, the prepared copolymer solutions were subjected to two different revolution per minute (RPM), i.e., (12, 60). Viscosity of the solutions was found inversely proportional to

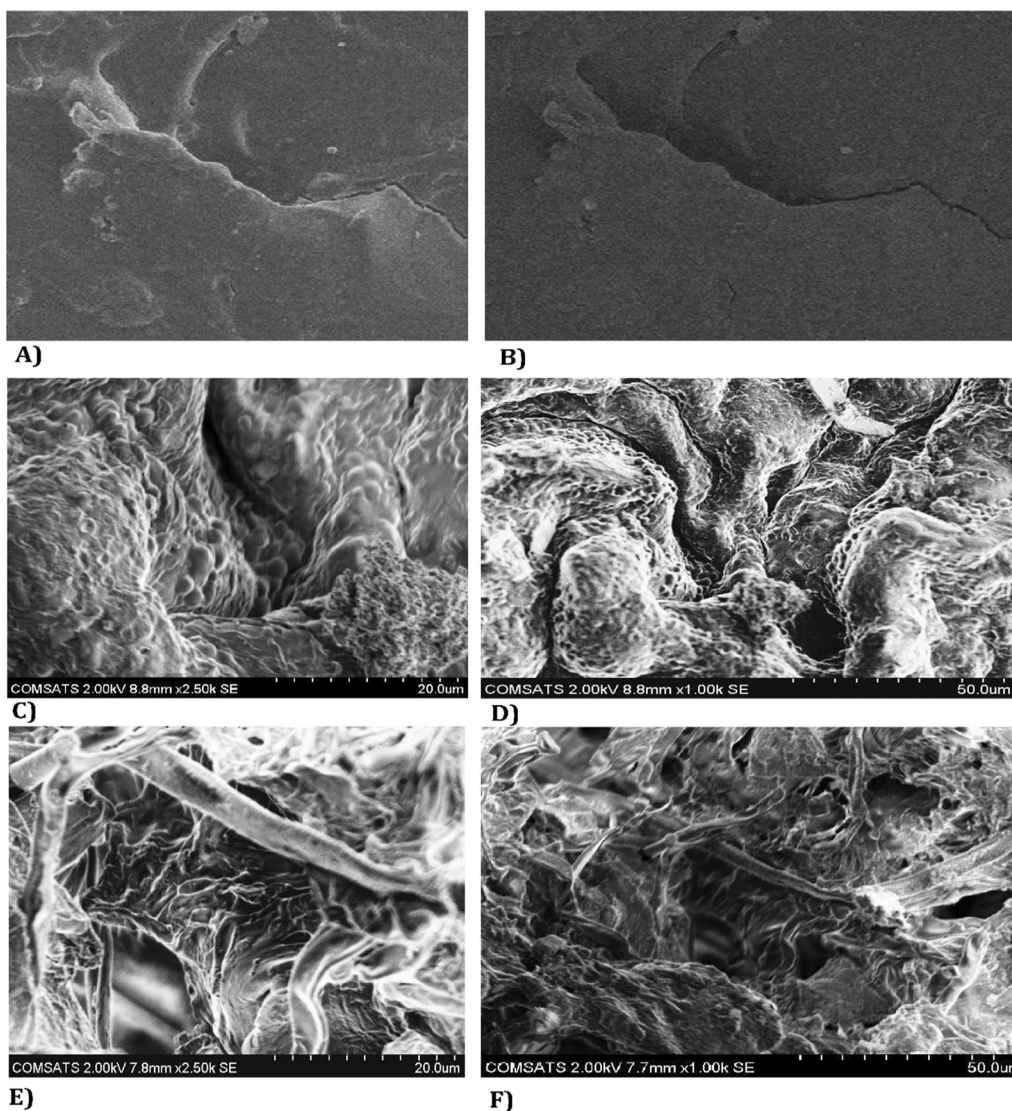


Fig. 7 Surface morphology of unloaded IPLVCS-2 copolymer hydrogel (A, B), cross-sectional morphologies of unloaded IPLVCS-2 copolymer hydrogel (C, D) drug-loaded IPLVCS-2 copolymer hydrogel (E, F)

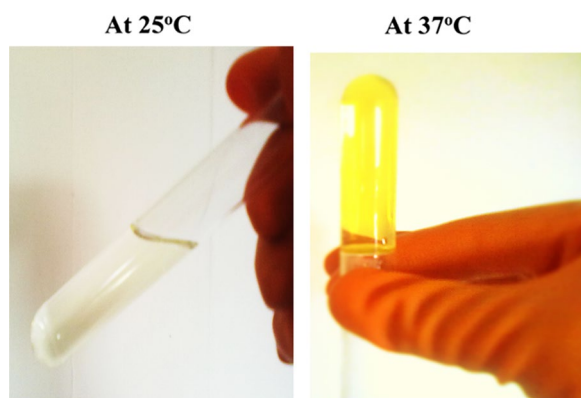


Fig. 8 Phase change behavior of poly (LVCS-g-PNIPAAm) hydrogels at room and physiological body temperature

the spindle speed (shear rate). By increasing the spindle speed, viscosity of the solutions was found to be decreased. Additional file 1: Table S1 indicates the effect of spindle speed at steady shear viscosity of copolymer solutions.

3.5 Rheological properties

3.5.1 Time sweep experiments

For the investigation of the viscoelastic nature of the poly (LVCS-g-PNIPAAm) in situ depot hydrogels with various feed ratios, the detailed gelation process was studied by using oscillatory rheometer. The rheological properties for the selected gel samples were measured by monitoring the viscosity, G' and G'' via conducting the time

sweep experiments. The oscillatory time sweep tests data are presented in Fig. 3 after mixing of the polymers and crosslinker.

Generally, G' represents the elastic behavior of formulations, while G'' refers to viscous state. From results, G'' was higher initially suggesting the sol state of the IPLVCS-1 (feed composition, 10:1.5 wt%) copolymer samples. With time elution, the buildup rate of G' becomes higher than G'' as gelation process proceeded and becomes equal near around 3 min. The point at which $G' = G''$ represents the crossover point which refers to the sol–gel change of samples. Beyond crossover point during the gelation process, the G' value becomes higher than G'' ($G' > G''$) representing the gel state of samples as demonstrated in Fig. 9A, B.

This response of samples with $G' > G''$ also indicates that elastic behavior of the sample dominates with the introduction of the covalent crosslinking with solid like behavior as in stable gel state. It is also known that elasticity of hydrogel sample can be predicted from its storage modulus, and generally increased storage modulus refers to a stable network with higher mechanical strength.

Moreover, it was investigated that with increasing LVCS contents (10:2 wt%), G' values of the samples increased as shown in Fig. 9B. This is suggested to be because of increased no of $-NH_2$ groups that take part in the crosslinking reactions and resulted in higher crosslinked density. The crossover point ($G' = G''$) for these samples was observed near around 2 min. Above this point, the G' value was found to be higher than G'' which indicates sol–gel state switch.

The effects of increasing crosslinking agent (GA) concentration on gelation behavior of the samples were also studied by monitoring the viscosity, G' and G'' . For crosslinking agent effect investigation, we select IPLVCS-5 and IPLVCS-6 samples with increasing GA concentrations. It was investigated from the data that with increasing GA concentrations, storage modulus (G') of the samples increases and crossover point was noted near around 2.5 min and 2.9 min for IPLVCS-5 and IPLVCS-6 samples, respectively. This increase in G' is suggested because of improved crosslinked density which occurs owing to higher polymerization reactions. Figure 9C, D indicates the change in gelation behavior of the samples with increasing GA concentrations.

3.5.2 Temperature sweep experiments

Figure 9E indicates the viscosities vs temperature profiles obtained for poly (LVCS-g-PNIPAAm) hydrogels. It was observed that the copolymer solutions showed a gradual viscosity increase with increasing temperature. This clearly indicates that the copolymer solution turned into gels form around the gelation temperatures which lies in

the vicinity of physiological temperature. Moreover, it was also observed that increasing the polymer concentration in copolymer solution compositions, viscosities sharply increased attaining the higher values at high polymer concentrations.

3.6 Optical transmittances

The change in optical transmittances for poly (LVCS-g-PNIPAAm) hydrogels was determined at variable measuring temperature using UV–visible spectrophotometer. Figure 9F shows the change in optical transmittances with temperature change. It was observed that with increasing temperature, colorless transparent copolymer solutions become opaque and resulted in decrease in transmittances. Moreover, with increasing LVCS contents, the crosslinking density increases during polymerization reactions, which further results in increased opaqueness of gels.

3.7 Determination of percent crosslinking

Glutaraldehyde was used as crosslinking agent for the formation of crosslinked copolymer depot hydrogels. It was noticed that by increasing the addition of NIPAAm into LVCS increased the percent crosslinking of copolymer hydrogels. This is suggested because by increasing polymeric contents, more functional groups are available for crosslinking and bonding, which in turn increased the % crosslinking of formulations. Table 2 and Fig. 10A refer to the percent crosslinking of synthesized in situ copolymer hydrogels.

3.8 Swelling test of poly (LVCS-g-PNIPAAm) hydrogels

3.8.1 Effect of temperature on swelling

Effect of temperature on swelling of poly (LVCS-g-PNIPAAm) hydrogels was studied at altered temperatures in pH = 2.1. Figure 10B, C shows the change in SR with increasing temperature of media. It was found that SR decreases with the increase of temperature of swelling media. The decrease in SR at high temperature is attributed to the collapse of PNIPAAm chains assuming a more hydrophobic state. The crosslinked PNIPAAm network consists of two regions, hydrophobic groups ($-CH(CH_3)_2$) and a hydrophilic region ($-CONH-$).

3.8.2 Oscillatory swelling–deswelling–reswelling cycles

Since the semi-in situ hydrogels swell differently at variable temperatures, the samples IPLVCS-2 and IPLVCS-5 were subjected to oscillatory swelling tests to investigate their temperature-dependent swelling reversibility. The reversibility process of temperature response for sample IPLVCS-2 between 25 and 37 °C is shown in Fig. 4D conducted at pH 2.1 at fixed time interval of 2 h. Figure 10D shows that with

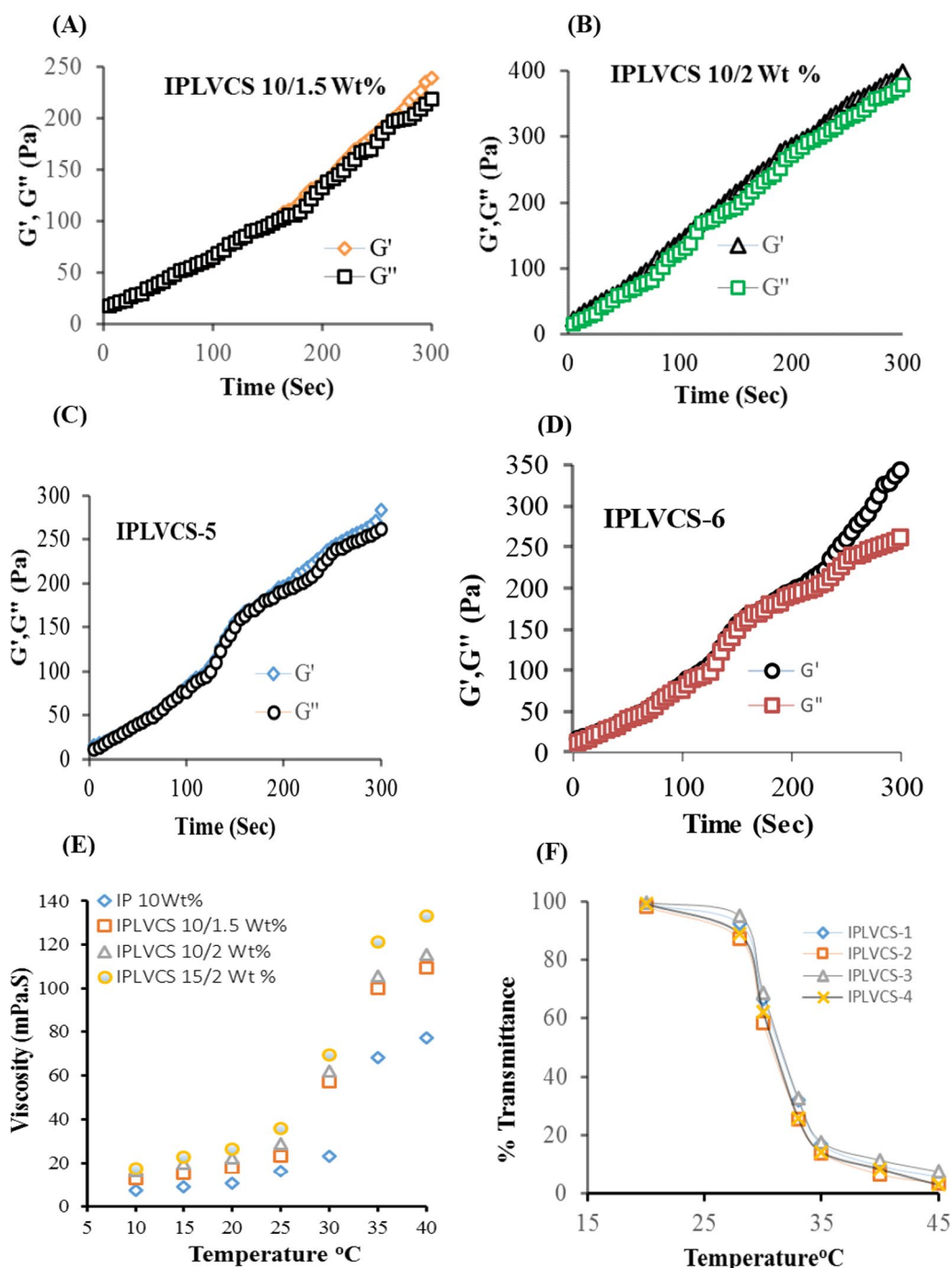


Fig. 9 Analysis of rheological behavior via monitoring of G' and G'' by conducting oscillatory time sweep test for poly (LVCS-*g*-PNIPAAm) in situ depot hydrogels at 30 °C (frequency, 1 Hz; strain = 1%). **A** Effect of LVCS contents (feed ratio 10/2 wt%) on G' and G'' . **B** Effect of crosslinking agent concentration (Glutaraldehyde) on G' and G'' . **C, D** Viscosities vs temperature profiles representing the gelation point at various concentrations for poly (N-isopropylacrylamide) (IP) alone and IPLVCS thermoresponsive in situ hydrogels ($n=3$, average \pm standard deviation). **E** Effect of temperature on optical transmittance of poly (LVCS-*g*-PNIPAAm) in situ depot hydrogels (**F**). Each point denotes the average \pm SD of $n=3$

increasing swelling and deswelling cycles, reversible response to temperature can be observed. This figure shows that the hydrogel swells and deswells with the

change of temperature and exhibits a good reversible behavior. The data shown in this figure do not represent the equilibrium swelling ratio (ESR). In poly

Table 2 Percent grafting efficiency, crosslinking and 5-FU-loaded (g/g) of poly (LVCS-g-PNIPAAm) in situ hydrogels ($n=3$)

Sample codes	% grafting efficiency	% crosslinking	5-FU-loaded (g/g)
IPLVCS-1	156	96.36	0.091
IPLVCS-2	168	97.47	0.087
IPLVCS-3	177	97.94	–
IPLVCS-4	198	98.42	0.068
IPLVCS-5	206	99.15	0.060
IPLVCS-6	219	99.70	0.052

(LVCS-g-PNIPAAm) hydrogels, LVCS provides the pores that facilitate the hydrogel network for the diffusion of water molecules.

3.8.3 Effect of pH on swelling

pH sensitivity of dual-responsive IPLVCS in situ depot hydrogels was studied in DW (PBS, 5 mM (pH=7.4) and pH=2.1 at variable temperatures. Figure 11A–C shows the effect of pH on swelling ratio (SR) of in situ hydrogels at different temperature programs. LVCS is a synthetic derivative of natural biopolymer (chitosan) which contain amino groups (NH₂) in its structure. It was observed from the dynamic swelling experiments shown in Fig. 11A–C that poly (LVCS-g-PNIPAAm) in situ depot hydrogels has highest swelling ratio (SR) in pH=2.1 below the Pka value of LVCS (6.3) as compared to 7.4.

Dynamic swelling of the poly (LVCS-g-PNIPAAm) depot hydrogels was also investigated in DW at different temperatures. Sample (IPLVCS-2) was selected to study the volume change response in DW. It is observed in Fig. 11A–C that poly (LVCS-g-PNIPAAm) in situ depot

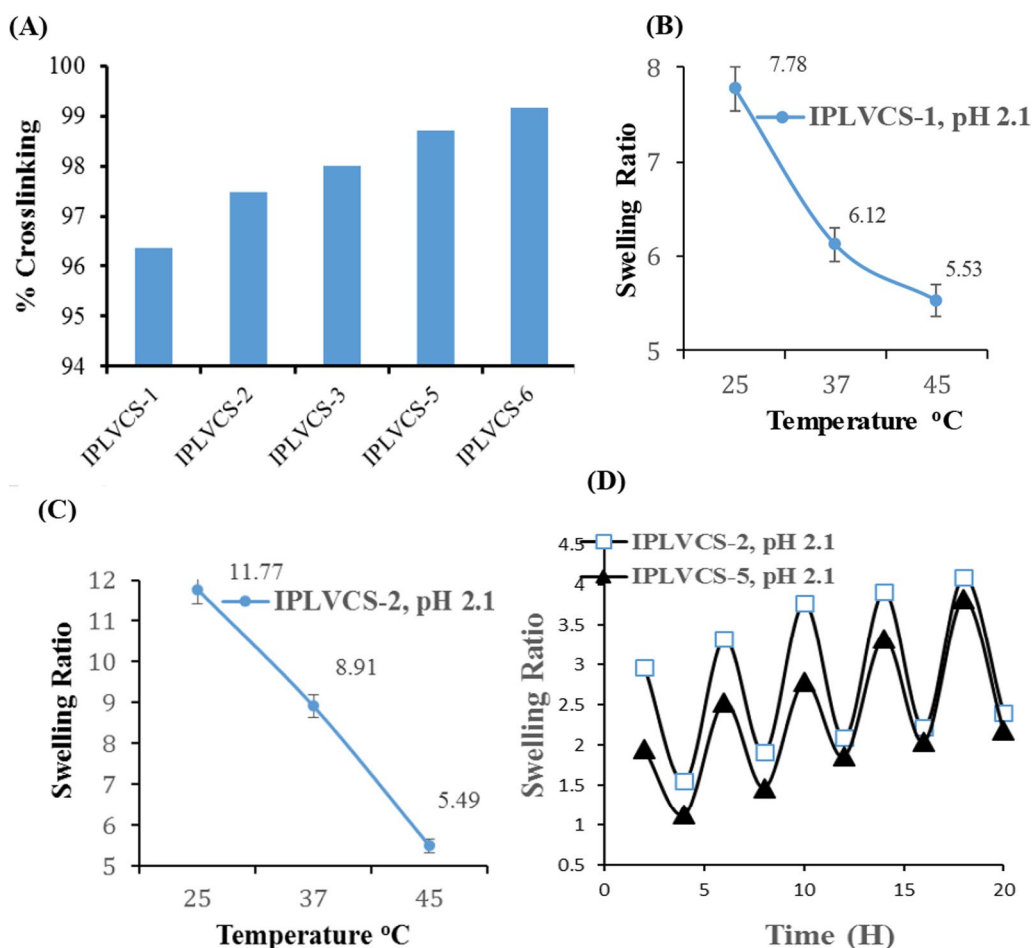


Fig. 10 Effect of polymeric and GA contents on % crosslinking of poly (LVCS-g-PNIPAAm) in situ hydrogels: (A) Effect of temperature and LVCS on ESR of poly (LVCS-g-PNIPAAm) depot hydrogels (B, C). Heating and cooling cycles IPLVCS-2 hydrogels at pH=2.1 between 25 and 37 °C (D). Each point shows the average ± SD of $n=3$

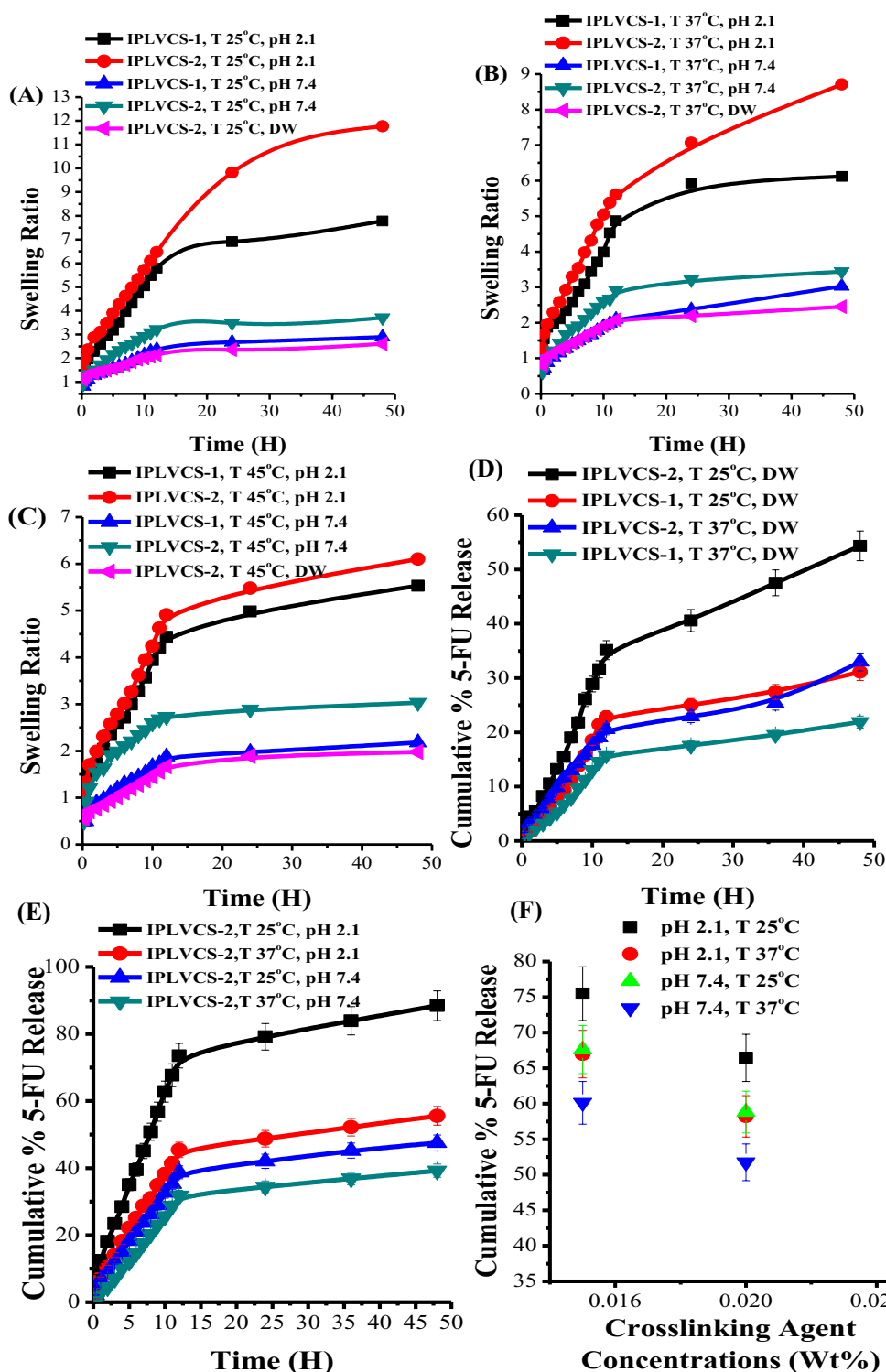


Fig. 11 Dynamic swelling behavior, pH and effect of increasing LVCS contents of the poly (LVCS-*g*-PNIPAAm) depot gels in buffered (pH=7.4, 5 mM and pH=2.1) and non-buffered media (DW) at **A** 25 °C, **B** 37 °C, **C** 45 °C. In vitro release from poly (LVCS-*g*-PNIPAAm) hydrogels in DW at different temperatures (**D**) pH and temperature effect on drug release from IPLVCS-2 in situ depot hydrogels at pH=2.1 (**E**). Effect of GA on in vitro release at different pH and temperatures (**F**). The data presented show mean ± SD (n=3)

hydrogels show no significant response to swelling process in DW. This behavior of poly (LVCS-g-PNIPAAm) depot hydrogels was suggested to be due the slight basic nature of DW (\sim pH=6.8) in which the amino groups of LVCS remain deprotonated. However, a slight response to volume change of hydrogel in DW was observed. This response to volume change was suggested owing to the hydrophilic nature of PNIPAAm. Additional file 1: Figure S2 shows the physical appearance of xerogel and swollen hydrogel discs in PBS (7.4) and pH=2.1.

3.8.4 Effect of LVCS on swelling

For poly (LVCS-g-PNIPAAm) depot hydrogels, it was noted that with increasing LVCS contents, i.e., IPLVCS-2 > IPLVCS-1, the in situ depot hydrogels show a highest swelling ratio (SR) in pH=2.1. Response of swelling behavior to increasing LVCS contents in various buffered and non-buffered media at different temperatures is shown in Fig. 11A–C.

3.8.5 In vitro drug release study from poly (LVCS-g-PNIPAAm) gels

Injectable depot formulations are easily controllable gels which control the release of drug via altering the material properties. Moreover, in targeting cancer tissues, the environment of the tumor may significantly affects drug release by providing pH and temperature-responsive properties in the formulations. For drug release study, drug-loaded hydrogel samples with (7×7 mm) in dimensions were selected, while samples IPLVCS-2, IPLVCS-5 and IPLVCS-6 were subjected to study the effect of GA on 5-FU release from hydrogels. Table 2 specifies the quantity of 5-FU-loaded in situ depot hydrogels.

3.8.5.1 Temperature and pH effect on drug release To study temperature and pH the effect on drug release, samples (IPLVCS-1 and IPLVCS-2) were selected due to its highest SR and LVCS contents. It was noted that poly (LVCS-g-PNIPAAm) gels have no significant response to drug release in DW and drug release was found to be $48 \pm 2.80\%$ for IPLVCS-2 and $30 \pm 1.63\%$ at 25 °C. This release in DW was suggested owing to presence of hydrophilic moieties in PNIPAAm. Moreover, at higher temperature (37 °C), drug release in DW was also found to be decreased accordingly for both samples. These results showed that with temperature increase, release of drug from the in situ gel matrix decreases, owing to the aggregated state at higher temperature [43]. Figure 11D indicates the cumulative % 5-FU release from IPLVCS-2 hydrogels in DW at variable temperature.

In vitro drug release from IPLVCS-2 hydrogels were also studied in PBS (pH=7.4) at two different temperatures. It was noted that in basic solutions (pH=7.4),

IPLVCS-2 showed a lesser drug release at both temperatures. Drug release at temperature 25 °C and pH=7.4 was found about $47 \pm 1.38\%$ and $37 \pm 1.25\%$ at 37 °C. This is because in PBS (7.4) the NH₂ groups in the gel network remain in deprotonated state, due to which the electrostatic repulsion between the polymer chains does not develop. This deprotonation of NH₂ groups in basic solutions leads to lesser swelling and drug release.

Alternatively, at pH=2.1, it was noted that there is a dramatic increase in the drug release from hydrogels at both temperatures, but the overall release of drug from hydrogels changes with the increase of temperature. This release in acidic solutions is suggested of protonated NH₂ groups in gel structure that leads to electrostatic repulsion. This repulsion between similar charge groups leads to chains expansion and drug release. The percent drug release was found to be $88 \pm 1.98\%$ at 25 °C and $55 \pm 1.94\%$ at 37 °C. Figure 11E indicates the response of IPLVCS-2 in situ hydrogels to 5-FU release at variable temperature and in solutions of various pH values.

3.8.5.2 Effect of crosslinking agent (GA) on drug loading and release Samples with codes IPLVCS-2 IPLVCS-5 and IPLVCS-6 were selected to investigate different GA concentration effect on drug loading and release. It was eminent from the results in Table 2 that loading of drug in in situ depot hydrogels decreases with the increasing concentrations of crosslinking agent in selected samples. This decreased loading of drug is suggested owing to compact structure of hydrogels.

The effect of GA concentrations on drug release was observed at pH (7.4, 2.1) and at variable temperatures as shown in Fig. 11F. It was noted that drug release from the gel samples decreases at both temperatures and pH values with the increasing GA ratios. This decrease in drug release was attributed mainly wing to increasing crosslinked density in the network structure. Moreover, in the crosslinking reactions of glutaraldehyde with the chitosan derivatives, most of the amino groups are consumed. The gel structure becomes more compact, and the mechanical strength of the hydrogels increases that leads to lesser diffusion of dissolution medium, swelling and drug release.

3.8.5.3 Effect of grafting efficiency percentage of PNIPAAm on 5-FU release Table 2 shows the percent grafting efficiency of the copolymer in situ hydrogels. The order of release of 5-FU from the gel matrix was IPLVCS-2 > IPLVCS-1 > IPLVCS-5 > IPLVCS-6. As shown in Table 2, drug loading and release from pH/thermo dual-responsive hydrogel matrix decreases with the increasing grafting of PNIPAAm. This can be explained by the fact that as the content of PNIPAAm and LVCS increases in the copoly-

mer chain, the chemical grafting reactions between the functional groups also increase. This leads to more compact structure and small pore size of the matrix which leads to difficult and slow diffusion of 5-FU molecules out of hydrogel matrix. Moreover, an increase in crosslinking agent ratio leads to increase in GE percentage, but it inversely decreases the release of 5-FU from gel matrix. This is also due to the increased crosslinking reactions between monomer and polymer functional groups that leads to compact structure of matrix and drug release. Moreover, no burst release was found for any hydrogel samples subjected to drug release experiments. This also indicates the important property of thermosensitive in situ hydrogel matrix system. Similar observations were found by Zhang et al. [41, 42].

3.8.5.4 Diffusion coefficient (D) Diffusion shows the penetration of fluids into the pre-existing voids in hydrogels. *D* values of poly (LVCS-g-PNIPAAm) hydrogels were calculated in acidic medium (pH=2.1). It was noted as in Additional file 1: Table S2 that “*D*” values of hydrogels decrease along with the increasing concentration of LVCS in the gel network. This is because poly (LVCS-g-PNIPAAm) hydrogels have highest swelling in acidic medium because of protonated -NH₂ groups in copolymer gel structure. Moreover, swelling process was also facilitated from the hydrophilic groups of PNIPAAm present in the copolymer structure. By increasing the concentration of crosslinking agent (IPLVCS-6 > IPLVCS-5), it was observed that “*D*” values increase owing to increased crosslinked density of the gel network that result in reduced pore size and slow diffusion of the solvent as shown in Additional file 1: Table S2.

3.8.6 *M_c* and (χ) parameter

Additional file 1: Table S2 indicates the *M_c* and χ values. It was observed that *M_c* values decrease with the increasing concentration of LVCS.

Solvent interaction parameters (χ) in acidic buffer solution (pH=2.1) were studied to examine the compatibility of polymers with fluids. Higher the (χ) values, weaker will be interaction forces between copolymers in gels and fluids. Additional file 1: Table S2 shows that (χ) values decrease with the increasing concentrations of LVCS in depot gels. This effect indicates that poly (LVCS-g-PNIPAAm) in situ depot hydrogels have strong interaction with the surrounding fluids. LVCS in the gel samples acts as channeling agents for solvent diffusion. It was also noted that (χ) values increase with the increasing concentrations of crosslinking agent. This might be owing to growing crosslinked density that reduces diffusion of the fluid.

3.8.7 Polymer volume fraction

V_{2,s} is used to investigate the hydrophilicity of gels. It was noted that volume fraction of the hydrogels increases with the increasing LVCS contents as shown in Additional file 1: Table S2. This effect suggests the hydrophilic character of the polymers and of thermoresponsive component, i.e., PNIPAAm. However, it was investigated that *V_{2,s}* decrease with increasing concentrations of GA. This effect shows the compact and denser network structure.

3.8.8 Drug release kinetics

The drug releases from poly (LVCS-g-PNIPAAm) depot hydrogels are governed by various parameters. These parameters mainly include solubility of drug in polymeric solution and water, diffusion of water into gel network, diffusion of drug from network and erosion of gel contents.

The regression coefficient (*R*²) values obtained showed that IPLVCS-2, IPLVCS-5 and IPLVCS-6 followed zero order with *R*² values near to 1 indicated in Tables 3 and 4 at both pH and temperature. These data show that drug release mechanism from the gels was pore diffusion controlled. These results also indicate that drug release from these formulations is not dependent on the

Table 3 Drug release kinetics from in situ hydrogels at 25 °C

Codes	pH	Zero model		First model		Higuchi model		Korsmeyer–Peppas model	
		<i>K₀</i> (h ⁻¹)	<i>R</i> ²	<i>K₁</i> (h ⁻¹)	<i>R</i> ²	<i>K₂</i> (h ⁻¹)	<i>R</i> ²	<i>n</i>	<i>R</i> ²
IPLVCS-2	2.1	5.693	0.997	0.101	0.974	22.87	0.970	0.728	0.988
	7.4	2.976	0.998	0.037	0.995	11.94	0.968	0.712	0.992
IPLVCS -5	2.1	4.123	0.999	0.057	0.989	16.48	0.962	0.852	0.993
	7.4	3.657	0.996	0.048	0.979	14.44	0.934	0.846	0.987
IPLVCS -6	2.1	3.549	0.999	0.046	0.992	14.14	0.955	0.837	0.995
	7.4	3.085	0.996	0.038	0.988	12.29	0.952	0.841	0.990

Table 4 Drug release kinetics at 37 °C

Sample codes	pH	Zero order		First order		Higuchi model		Korsmeyer–Peppas model	
		K_0 (h ⁻¹)	R^2	K_1 (h ⁻¹)	R^2	K_2 (h ⁻¹)	R^2	n	R^2
IPLVCS-2	2.1	3.591	0.994	0.047	0.997	14.53	0.981	0.888	0.975
	7.4	2.618	0.998	0.031	0.991	10.36	0.943	0.902	0.925
IPLVCS-5	2.1	3.664	0.997	0.047	0.986	14.56	0.949	0.995	0.980
	7.4	3.331	0.994	0.042	0.981	13.23	0.945	0.908	0.977
IPLVCS-6	2.1	3.177	0.998	0.040	0.996	12.74	0.967	0.912	0.947
	7.4	2.673	0.996	0.034	0.997	10.73	0.968	0.869	0.977

drug concentration in gel network. The value of release exponent “*n*” was obtained by applying Korsmeyer–Peppas model to examine mechanism of release. The “*n*” values shown in Tables 3 and 4 were found more than 0.5 at both temperature programs. The data indicates that 5-FU release from gels occur via non-Fickian mechanism specifying swelling and relaxation phenomena.

3.8.9 Cell culture experiments

3.8.9.1 In vitro cytocompatibility study of poly (LVCS-g-PNIPAAm) in situ depot hydrogels In vitro cytocompatibility of gels was proven by MTT assay against Vero cell lines, and the graph is explained in Fig. 12. The untreated cells used as negative control showed 95% viability. From Fig. 12A it is very clear that there is no prominent difference in cell viability (%) between the negative control and the cells treated with in situ copolymer hydrogels (100 mg/ml). However, cells preserved with Triton-X 100 exterminated the cells which show its toxic nature. This confirms the cytocompatibility of PNIPAAm-based pH/thermo dual-responsive hydrogels with no detectable cytotoxicity. Therefore, copolymer in situ forming hydrogels can be considered as safe drug delivery controlled delivery depot. Table 5 indicates the % cell inhibition of copolymer in situ hydrogels in Vero cell lines.

3.8.9.2 In vitro anticancer activity of 5-FU-loaded in situ depot hydrogels *IC*₅₀ values evaluation MTT assay was used to find the number of surviving cells. Figure 12B represents the MTT sketch of 5-FU pure solution and 5-FU-loaded in situ gels for concentrations from (1, 5, 10, 20, 40, 60, 80 and 100 µg/mL) in MCF-7 cell line. It is clear from the graphs that the anticancer activity of 5-FU-loaded gels was dose dependent. MCF-7 cells incubated with a higher dose exhibited higher cell death compared to the lower dose. It is clear from Fig. 6B that with increased concentration gradient per well of 5-FU-loaded copolymer hydrogels, % cell viability decreased accordingly. Also

from Fig. 12B, it was concluded that 5-FU retains its anti-cancer activity toward MCF-7 cells even after incorporating in to the pH/thermo dual-responsive in situ gels. The effects of treatment are presented as percentages of viable cells with respect to untreated control cells.

The *IC*₅₀ values were calculated from dose–response curves shown in Fig. 6C. *IC*₅₀ values were found increased in the following order: IPLVCS-2 (47 ± 1 µg/ml), IPLVCS-6 (34 ± 17 µg/ml) and free 5-FU (52 ± 3 µg/ml). These results confirmed that MCF-7 cells might have more sensitivity to 5-FU-loaded copolymer gels as compared to free 5-FU solution. Table 5 shows *IC*₅₀ calculated for pure 5-FU and loaded in in situ copolymer hydrogels (IPLVCS-2, IPLVCS-6). 5-FU in cells may induce cell death or injury by two possible mechanisms. 5-FU brought cell death in cancer cells either through inhibition of thymidylate which is essential for the synthesis of DNA. The deficiency of this component leads to the inhibition of cell division and cell death. Cell death in cancer cells also supposed to be caused by the metabolic error, in which nuclear transcriptional enzymes replace the uridine triphosphate (UTP) mistakenly by 5-fluorouridine triphosphate (FUTP). This metabolic error leads to the cell apoptosis or death by interfering with RNA processing and protein synthesis.

4 Discussion

In the current study, a series of PNIPAAm-based in situ forming depot hydrogels were synthesized using cold method with LVCS. NMR and FTIR confirmed the structure formation of hydrogels, while TGA DSC showed the stable thermal nature of developed hydrogels. Moreover, from SEM analysis, it was found that hydrogels have porous nature which facilitates the uptake and release of drug. For in situ depot hydrogels, one of the important factors to consider is their sol–gel phase transition. It was found from results that the gelation temperature and time of the in situ formulations decrease with the increase of

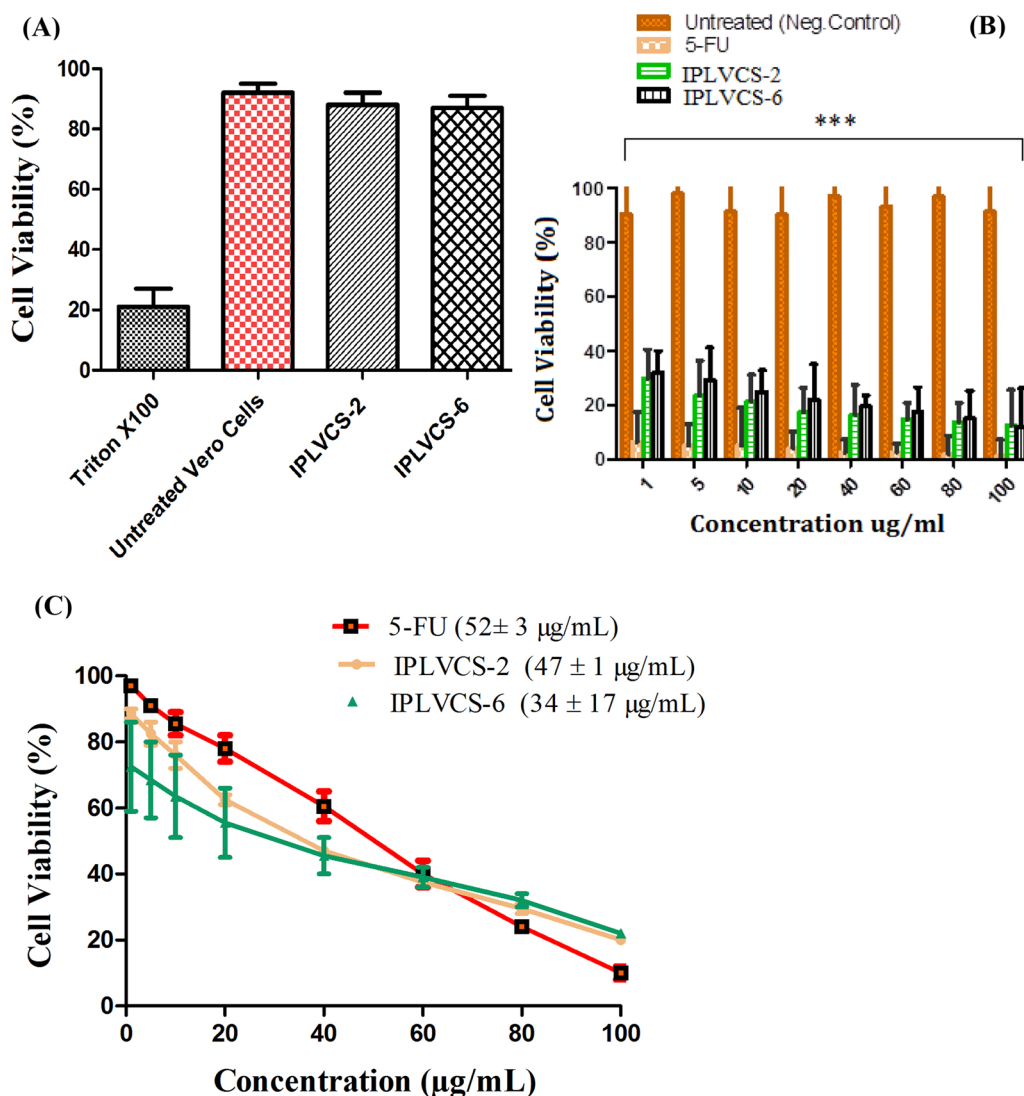


Fig. 12 In vitro cytocompatibility of poly (LVCS-*g*-PNIPAAm) depot gels against Vero cells **(A)** In vitro cytotoxicity of 5-FU-loaded poly (LVCS-*g*-PNIPAAm) depot gels in MCF-7 cancer cells **(B)** dose–response curves for IC₅₀ values determination **(C)**. Data specify the mean ± SD (*n*=3) with statistical significance ****p* value of <0.0001

Table 5 IC₅₀ values and % inhibition of pure free 5-FU and 5-FU encapsulated hydrogels against MCF-7 and Vero cells

Sample codes	IC ₅₀ (µg/ml) ^a	% cell inhibition ± SEM in Vero cells
5-FU	52 ± 3	89 ± 3.11
IPLVCS-2	47 ± 1	12 ± 2.04
IPLVCS-6	34 ± 17	13 ± 2.31

NIPAAm concentration. With the increase in PNIPAAm concentration, a progressive decrease in gelation temperature was observed shown in Table 1. This decrease in

temperature is suggested of dominant hydrophobic effect of isopropyl groups in the network chain. It is also noted that with LVCS increase in feed ratio of gels (IPLVCS-1 and IPLVCS-2), the gelation temperature increases as shown in Table 1. It is suggested because of the presence of high NH₂ hydrophilic groups, which causes hydrophilic interactions and in turn require high temperature and time for water evaporation. This in turn leads to high temperature and time for gelation with LVCS contents increase. The results from samples IPLVCS-4 and IPLVCS-5 show that increasing of GA contents has no major effect on the gelation temperature. However, decrease in gelation time was noted with increasing

GA concentration. This is suggested because of higher crosslinking reactions. The viscoelastic nature of the poly (LVCS-g-PNIPAAm) in situ depot hydrogels with various feed ratios was studied with rheological analysis. From time sweep experiments, it was concluded that with time elution and increasing LVCS and GA contents, $G' > G''$ was observed which showed the dominant elastic state with the introduction of the covalent crosslinking and stable gel state. Moreover, from temperature experiments, it was noted that with increasing temperature, a sharp change in viscosity was observed which showed the transition into gels state. From optical transmittance it was noted that with temperature variation, a change in transparency was noted. However, this decrease in transparency of the gels with increasing polymeric contents were not significant below LCST of the gels. However, it was observed that above LCST (near 33 °C), all the in situ depot gels exhibited a sharp increase in the opaqueness with a small difference among the gel samples. Moreover, an increase in percent crosslinking was noted owing to increase of monomer or polymer contents in the structure. The presence of higher contents of monomer or polymers in gel network provides more functional groups to be available for grafting reactions that in turn increase the percent crosslinking. From swelling experiments it was noted that SR decreased with increasing temperature. At lower temperature < LCST of hydrogels, the hydrophilic groups from the PNIPAAm form an intermolecular hydrogen bond with the surrounding water allow them to penetrate into gel network and leads to increased SR. The water molecules at low temperature are in bound state with the gel backbone leading to diffusion and in turn swelling of hydrogels. With the increase of temperature, the water molecules gain an enthalpy. The hydrophobic interactions between the hydrophobic groups of PNIPAAm increase. As a result, some of the hydrogen bonds are broken with the subsequent expulsion of water from network. This release of water from gel network leads to the decrease in SR [31]. Moreover, higher swelling was observed at pH = 2.1. This is because at low pH (2.1) below the Pka value of buffer solution, amino groups (NH_2) of LVCS get ionized and converted to ($-\text{NH}^{+3}$). These large numbers of protonated amino groups with similar charges at low pH cause electrostatic repulsion and chains expansion, which leads to hydrogels swelling. On the other hand, it was observed that swelling of the hydrogels decreases in buffer solutions of higher pH value, i.e., (7.4). This is because, at high pH value, the protonated amino groups become deprotonated. This deprotonation leads to the excretion of repulsion which leads to the decrease in SR [11]. Moreover, with increasing LVCS contents increased in SR was found owing to presence of number of protonated amino groups in

copolymer chain increases. This protonation develops an increased electrostatic repulsion in hydrogel network which leads to increase swelling ratio (SR). The results become inverse in solutions of high pH values (7.4) owing to deprotonation of (NH_2) groups in the polymer chains. Similarly from in vitro release experiments, it was found that higher release of drug was noted at lower temperature and acidic pH which correlates with the swelling behavior of gels. Additionally it was also noted that, with increasing GA contents, drug loading and release from samples decreased. It was noted that drug release from the gel samples decreases at both temperatures and pH values with the increasing GA ratios. This decrease in drug release was attributed mainly wing to increasing crosslinked density in the network structure. Moreover, in the crosslinking reactions of glutaraldehyde with the chitosan derivatives, most of the amino groups are consumed. The gel structure becomes more compact and the mechanical strength of the hydrogels increases that leads to lesser diffusion of dissolution medium, swelling and drug release. Moreover, different networking parameters have different effects on hydrogels. It was noted that D' values of hydrogels decrease along with the increasing concentration of LVCS, while D values increased with GA contents. Similarly M_c values decreases with the increasing LVCS. This is because increasing concentration of LVCS provides large number of NH_2 groups which get consumed during the polymerization reactions and result in reduced M_c values. Moreover, (χ) values decreases with the increasing concentrations of LVCS in depot gels. This effect indicates that poly (LVCS-g-PNIPAAm) in situ depot hydrogels have strong interaction with the surrounding fluids, while $V_{2,s}$ values increased with GA contents which shows the compact and denser network structure. From release kinetics, it was found that depot gels exhibited zero order and non-Fickian mechanism. MTT assay confirmed the cytocompatibility of hydrogels against Vero cells. Moreover, the anticancer activity against MCF-7 cells showed that depot gels exhibited dose dependent cells death in gels depot form.

5 Conclusion

The main objective of the current study was to increase the bioavailability of 5-FU based on the hypothesis of developing pH/thermo dual-responsive injectable intratumoral depot hydrogels. Tube titling experiments confirmed sol-gel phase change of formulations with temperature. Oscillatory time experiments showed that the depot formulations have viscoelastic properties. The swelling experiments showed that IPLVCS in situ hydrogels have significant pH sensitivity with highest SR in acidic environment and at 25 °C owing to electrostatic repulsion between similar protonated groups (NH_2).

Oscillatory heating and cooling cycles showed that temperature causes significant structural changes in the responsive hydrogels and effect the swelling and drug release pattern from hydrogels might be due to the relaxation and collapsing of network chains. The *in vitro* drug release profile showed that developed depot gels have potential pH/thermo responsive nature with sustained release properties. The highest *in vitro* 5-FU release ($88 \pm 1.98\%$) was found in acidic media, i.e., pH 2.1 and at 25 °C for IPLVCS-2 *in situ* hydrogel. Results concluded that increased chemical grafting and crosslinking between the functional groups reduces the 5-FU release from the pH/thermo responsive hydrogel matrix owing to more compact structure. Different networking parameters (D , M_c , V_{2S} and χ) calculated through Flory–Rhener theory showed that the porous nature and mesh size (crosslinked density) affect the swelling and drug release. Release kinetic study showed that the developed *in situ* depot gels follow zero order with non-Fickian mechanism. MTT assay showed that *in situ* depot hydrogels with tunable pH/thermo properties has significant cytocompatibility and cytotoxicity against Vero and MCF-7 cells. The IC_{50} values confirmed that 5-FU has highest inhibition in depot form as compared to free form. NMR and FTIR spectroscopy confirmed gel network formation. TGA and DSC proved the thermal stability of *in situ* depot hydrogels over an extended temperature range. SEM micrographs showed the porous nature of the hydrogels. It was concluded that low viscous chitosan (LVCS) with abundant NH_2 groups in its side chain provides significant pH sensitivity to poly (LVCS-g-PNIPAAm) *in situ* depot injectable hydrogels with tunable thermosensitive properties. The current findings exhibited that 5-FU-loaded *in situ* hydrogels act as drug depot and capable of providing controlled release after intratumoral injection, in so doing improving its chemotherapeutic effect in various cancer types in comparison to existing treatment types while reducing its systemic toxicity.

6 Supporting information

General representation of (A) pH responsive (B) Temperature responsive (C) pH/Thermo dual responsive hydrogels; Temperature dependence optical transmittance (450 nm) of pH/Thermo dual responsive injectable depot hydrogels; Photographs of the Xerogel and Swollen hydrogel discs in swelling media of variable pH values; Viscosity $[\eta]$ of copolymer solutions at variable shear rates; Diffusion Coefficient (D) and Networking Parameters of pH/Thermo dual responsive *in situ* depot hydrogels.

Abbreviations

5-FU	5-Fluorouracil
LVCS	Low viscous grade chitosan
PNIPAAm	Poly(<i>N</i> -isopropylacrylamide)
MTT	Methyl thiazolyl tetrazolium assay
NMR	Nuclear magnetic resonance
FTIR	Fourier transform infrared spectroscopy
TGA	Thermogravimetric analysis
DSC	Differential scanning calorimetry
SEM	Scanning electron microscopy
GA	Glutaraldehyde
LCST	Lower critical solution temperature

Supplementary Information

The online version contains supplementary material available at <https://doi.org/10.1186/s43088-023-00459-5>.

Additional file 1. Supplementary figures and tables.

Acknowledgements

Authors would like to acknowledge Hong Kong Special Administrative Region (HKSAR) Government and InnoHK for providing conducive work environment in data documentation.

Author contributions

All authors contributed equally in this study. SK and BK designed and conducted experiments. HL wrote the initial draft of study. SK reviewed and approved the final draft.

Funding

No funding is obtained for the study.

Availability of data and materials

All data generated are included in this article.

Declarations

Ethics approval and consent to participate

Not applicable.

Consent for publication

Not applicable.

Competing interest

No potential conflict of interest was reported.

Author details

¹Centre for Eye and Vision Research, 17W Science Park, Shatin, Hong Kong, China. ²Hong Kong Center of Cerebro-Cardiovascular Engineering, 19W Science Park, Shatin, Hong Kong, China. ³School of Optometry, The Hong Kong Polytechnic University, Kowloon, Hong Kong SAR, China. ⁴Department of Biomedical Engineering, City University Hong Kong, Kowloon, Hong Kong SAR, China.

Received: 22 May 2023 Accepted: 11 December 2023

Published online: 19 December 2023

References

1. Bukhari SMH, Khan S, Rehanullah M, Ranjha NM (2015) Synthesis and characterization of chemically cross-linked acrylic acid/gelatin hydrogels: effect of pH and composition on swelling and drug release. *Int J Polym Sci* 2015:1–15. <https://doi.org/10.1155/2015/187961>

2. Chen LQ, Pagel MD (2015) Evaluating pH in the extracellular tumor micro-environment using CEST MRI and other imaging methods. *Adv Radiol* 2015:1–25. <https://doi.org/10.1155/2015/206405>
3. Choi C, Chae SY, Nah J-W (2006) Thermosensitive poly(N-isopropylacrylamide)-b-poly(ϵ -caprolactone) nanoparticles for efficient drug delivery system. *Polymer (Guildf)* 47:4571–4580. <https://doi.org/10.1016/j.polymer.2006.05.011>
4. Choi IS, Oh D-Y, Kim B-S, Lee K-W, Kim JH, Lee J-S (2007) Oxaliplatin, 5-FU, folinic acid as first-line palliative chemotherapy in elderly patients with metastatic or recurrent gastric cancer. *Cancer Res Treat* 39:99–103. <https://doi.org/10.4143/crt.2007.39.3.99>
5. Delair T (2012) In situ forming polydisaccharide-based 3D-hydrogels for cell delivery in regenerative medicine. *Carbohydr Polym* 87:1013–1019. <https://doi.org/10.1016/j.carbpol.2011.09.069>
6. Ekensear AK, Boere KWM, Tzouanas SN, Vo TN, Kasper FK, Mikos AG (2012) Synthesis and characterization of thermally and chemically gelling injectable hydrogels for tissue engineering. *Biomacromol* 13:1908–1915. <https://doi.org/10.1021/bm300429e>
7. Fundueanu G, Constantin M, Bucatariu S, Ascenzi P (2017) pH/thermo-responsive poly(N-isopropylacrylamide-co-maleic acid) hydrogel with a sensor and an actuator for biomedical applications. *Polymer (Guildf)* 110:177–186. <https://doi.org/10.1016/j.polymer.2017.01.003>
8. Gao X, Zhou Y, Ma G, Shi S, Yang D, Lu F, Nie J (2010) A water-soluble photocrosslinkable chitosan derivative prepared by Michael-addition reaction as a precursor for injectable hydrogel. *Carbohydr Polym* 79:507–512. <https://doi.org/10.1016/j.carbpol.2009.08.033>
9. Günzburg WH, Löhr M, Salmons B (2002) Novel treatments and therapies in development for pancreatic cancer. *Expert Opin Investig Drugs* 11:769–786. <https://doi.org/10.1517/13543784.11.6.769>
10. Guo B-L, Gao Q-Y (2007) Preparation and properties of a pH/temperature-responsive carboxymethyl chitosan/poly(N-isopropylacrylamide)/semi-IPN hydrogel for oral delivery of drugs. *Carbohydr Res* 342:2416–2422. <https://doi.org/10.1016/j.carres.2007.07.007>
11. He G, Zheng H, Xiong F (2008) Preparation and swelling behavior of physically crosslinked hydrogels composed of poly(vinyl alcohol) and chitosan. *J Wuhan Univ Technol Sci Ed* 23:816–820. <https://doi.org/10.1007/s11595-007-6816-1>
12. Ilson DH (2003) Oesophageal cancer: new developments in systemic therapy. *Cancer Treat Rev* 29:525–532. [https://doi.org/10.1016/S0305-7372\(03\)00104-X](https://doi.org/10.1016/S0305-7372(03)00104-X)
13. Jankaew R, Rodkate N, Lamlerthton S, Rutnakornpituk B, Wichai U, Ross G, Rutnakornpituk M (2015) “Smart” carboxymethylchitosan hydrogels crosslinked with poly(N-isopropylacrylamide) and poly(acrylic acid) for controlled drug release. *Polym Test* 42:26–36. <https://doi.org/10.1016/j.polymertesting.2014.12.010>
14. Jemal A, Siegel R, Ward E, Hao Y, Xu J, Murray T, Thun MJ (2008) Cancer statistics, 2008. *CA Cancer J Clin* 58:71–96. <https://doi.org/10.3322/CA.2007.0010>
15. Khan S, Akhtar N, Minhas MU, Badshah SF (2019) pH/thermo-dual responsive tunable in situ cross-linkable depot injectable hydrogels based on poly(N-isopropylacrylamide)/carboxymethyl chitosan with potential of controlled localized and systemic drug delivery. *AAPS PharmSciTech*. <https://doi.org/10.1208/s12249-019-1328-9>
16. Khan S, Minhas MU, Ahmad M (2017) Self-assembled supramolecular thermoreversible β -cyclodextrin/ethylene glycol injectable hydrogels with difunctional Pluronic 127 as controlled delivery depot of curcumin. Development, characterization and in vitro evaluation. *J Biomater Sci Polym Ed* 5063:1–34. <https://doi.org/10.1080/09205063.2017.1396707>
17. Khan S, Minhas MU, Akhtar N, Thakur RRS (2022) Sodium alginate/N-(Vinylcaprolactam) based supramolecular self-assembled subcutaneously administered in situ formed gels depot of 5-fluorouracil: rheological analysis, in vitro cytotoxic potential, in vivo bioavailability and safety evaluation. *Int J Biol Macromol* 211:425–440. <https://doi.org/10.1016/J.IJBIOMAC.2022.05.035>
18. Khan S, Ranjha NM (2014) Effect of degree of cross-linking on swelling and on drug release of low viscous chitosan/poly(vinyl alcohol) hydrogels. *Polym Bull* 71:2133–2158
19. Ko DY, Shinde UP, Yeon B, Jeong B (2013) Recent progress of in situ formed gels for biomedical applications. *Prog Polym Sci* 38:672–701. <https://doi.org/10.1016/j.progpolymsci.2012.08.002>
20. Li Y, Rodrigues J, Tomás H (2012) Injectable and biodegradable hydrogels: gelation, biodegradation and biomedical applications. *Chem Soc Rev* 41:2193–2221. <https://doi.org/10.1039/c1cs15203c>
21. Li Z, Shen J, Ma H, Lu X, Shi M, Li N, Ye M (2012) Preparation and characterization of pH- and temperature-responsive hydrogels with surface-functionalized graphene oxide as the crosslinker. *Soft Matter* 8:3139. <https://doi.org/10.1039/c2sm07012j>
22. Lin H-M, Wang W-K, Hsiung P-A, Shyu S-G (2010) Light-sensitive intelligent drug delivery systems of coumarin-modified mesoporous bioactive glass. *Acta Biomater* 6:3256–3263. <https://doi.org/10.1016/j.actbio.2010.02.014>
23. Liu C, Yu J, Jiang G (2013) Thermosensitive poly (N-isopropylacrylamide) hydrophobic associated hydrogels: optical, swelling/deswelling, and mechanical properties. *J Mater Sci*. <https://doi.org/10.1007/s10853-012-6794-3>
24. Moehler M, Teufel A, Galle PR (2005) New chemotherapeutic strategies in colorectal cancer. *Recent Results Cancer Res. Fortschritte der Krebsforsch. Prog. dans les Rech. sur le cancer* 165, 250–259
25. Nasir F, Iqbal Z, Khan JA, Khan A, Khuda F, Ahmad L, Khan A, Khan A, Dayoo A (2012) Development and evaluation of diclofenac sodium thermoreversible subcutaneous drug delivery system. *Int J Pharm* 439:120–126. <https://doi.org/10.1016/j.ijpharm.2012.10.009>
26. Nishiyama M, Eguchi H (2009) Pharmacokinetics and pharmacogenomics in gastric cancer chemotherapy. *Adv Drug Deliv Rev* 61:402–407. <https://doi.org/10.1016/J.ADDR.2008.09.004>
27. Overstreet DJ, Dutta D, Stabenfeldt SE, Vernon BL (2012) Injectable hydrogels. *J Polym Sci Part B Polym Phys* 50:881–903. <https://doi.org/10.1002/polb.23081>
28. Park K-H, Song H-C, Na K, Bom H-S, Lee KH, Kim S, Kang D, Lee DH (2007) Ionic strength-sensitive pullulan acetate nanoparticles (PAN) for intratumoral administration of radioisotope: ionic strength-dependent aggregation behavior and (99m)Technetium retention property. *Colloids Surf B Biointerfaces* 59:16–23. <https://doi.org/10.1016/j.colsurfb.2007.04.010>
29. Rodkate N, Rutnakornpituk B, Wichai U, Ross G, Rutnakornpituk M (2015) Smart carboxymethylchitosan hydrogels that have thermo- and pH-responsive properties. *J Appl Polym Sci*. <https://doi.org/10.1002/app.41505>
30. Shah HS, Al-Oweini R, Haider A, Kortz U, Iqbal J (2014) Cytotoxicity and enzyme inhibition studies of polyoxometalates and their chitosan nanoassemblies. *Toxicol Rep* 1:341–352. <https://doi.org/10.1016/j.toxrep.2014.06.001>
31. Shekhar S, Mukherjee M, Sen AK (2015) Swelling, thermal and mechanical properties of NIPAM-based terpolymeric hydrogel. *Polym Bull* 73:125–145. <https://doi.org/10.1007/s00289-015-1476-3>
32. Sohail M, Ahmad M, Minhas MU, Ali L, Khalid I, Rashid H (2015) Controlled delivery of valsartan by cross-linked polymeric matrices: synthesis, in vitro and in vivo evaluation. *Int J Pharm* 487:110–119. <https://doi.org/10.1016/j.ijpharm.2015.04.013>
33. Tamer TM, Omer AM, Hassan MA, Hassan ME, Sabet MM, Eldin MSM (2015) Development of thermo-sensitive poly N-isopropyl acrylamide grafted chitosan derivatives
34. Wan Ngah W, Endud C, Mayanar R (2002) Removal of copper(II) ions from aqueous solution onto chitosan and cross-linked chitosan beads. *React Funct Polym* 50:181–190. [https://doi.org/10.1016/S1381-5148\(01\)00113-4](https://doi.org/10.1016/S1381-5148(01)00113-4)
35. Wang B, Wu X, Li J, Hao X, Lin J, Cheng D, Lu Y (2016) Thermosensitive behavior and antibacterial activity of cotton fabric modified with a chitosan-poly (N-isopropylacrylamide) interpenetrating polymer network hydrogel. *Polymers*. <https://doi.org/10.3390/polym8040110>
36. Wei H, Cheng S-X, Zhang X-Z, Zhuo R-X (2009) Thermo-sensitive polymeric micelles based on poly(N-isopropylacrylamide) as drug carriers. *Prog Polym Sci* 34:893–910. <https://doi.org/10.1016/j.progpolymsci.2009.05.002>
37. Whiteside TL (2008) The tumor microenvironment and its role in promoting tumor growth. *Oncogene* 27:5904–5912. <https://doi.org/10.1038/onc.2008.271>
38. Wu W, Shen J, Banerjee P, Zhou S (2010) Chitosan-based responsive hybrid nanogels for integration of optical pH-sensing, tumor cell imaging and controlled drug delivery. *Biomaterials* 31:8371–8381. <https://doi.org/10.1016/j.biomaterials.2010.07.061>

39. Xiong W, Wang W, Wang Y, Zhao Y, Chen H, Xu H, Yang X (2011) Dual temperature/pH-sensitive drug delivery of poly(N-isopropylacrylamide-co-acrylic acid) nanogels conjugated with doxorubicin for potential application in tumor hyperthermia therapy. *Colloids Surf B Biointerfaces* 84:447–453. <https://doi.org/10.1016/j.colsurfb.2011.01.040>
40. Yarden Y, Baselga J, Miles D (2004) Molecular approach to breast cancer treatment. *Semin Oncol* 31:6–13. <https://doi.org/10.1053/J.SEMINONCOL.2004.07.016>
41. Zhang L, Wang L, Guo B, Ma PX (2014) Cytocompatible injectable carboxymethyl chitosan/N-isopropylacrylamide hydrogels for localized drug delivery. *Carbohydr Polym* 103:110–118. <https://doi.org/10.1016/j.carbpol.2013.12.017>
42. Zhang Y, Gao C, Li X, Xu C, Zhang Y, Sun Z (2014) Thermosensitive methyl cellulose-based injectable hydrogels for post-operation anti-adhesion. *Carbohydr Polym* 101:171–178. <https://doi.org/10.1016/j.carbpol.2013.09.001>
43. Zhao SP, Li LY, Cao MJ, Xu WL (2011) PH- and thermo-sensitive semi-IPN hydrogels composed of chitosan, N-isopropylacrylamide, and poly(ethylene glycol)-co-poly(ϵ -caprolactone) macromer for drug delivery. *Polym Bull* 66:1075–1087. <https://doi.org/10.1007/s00289-010-0390-y>
44. Zhou X, Wang J, Nie J, Du B (2016) Poly(N-isopropylacrylamide)-based ionic hydrogels: synthesis, swelling properties, interfacial adsorption and release of dyes. *Polym J*. <https://doi.org/10.1038/pj.2015.123>

Publisher's Note

Springer Nature remains neutral with regard to jurisdictional claims in published maps and institutional affiliations.

Submit your manuscript to a SpringerOpen[®] journal and benefit from:

- Convenient online submission
- Rigorous peer review
- Open access: articles freely available online
- High visibility within the field
- Retaining the copyright to your article

Submit your next manuscript at ► [springeropen.com](https://www.springeropen.com)
